Ruthenium Complexes Containing Two Ru−(η^2-Si−H) Bonds: Synthesis, Spectroscopic Properties, Structural Data, Theoretical Calculations, and Reactivity Studies

Fabien Delpech,[†] **Sylviane Sabo-Etienne,*,†** **Jean-Claude Daran,**[†] **Bruno Chaudret,**[†] **Khansaa Hussein,**[‡,§] **Colin J. Marsden,**[‡] **and Jean-Claude Barthelat**[‡]

Laboratoire de Chimie de Coordination du CNRS, 205 route de Narbonne, 31077 Toulouse Cedex 04, France, and Laboratoire de Physique Quantique, IRSAMC (UMR 5626), Université Paul Sabatier, 118 route de Narbonne, 31062 Toulouse Cedex 4, France

Received January 20, 1999

Abstract: The bis(dihydrogen) complex RuH$_2$(H$_2$)$_2$(PCy$_3$)$_2$ (**1**) reacts with the disilanes (R$_2$SiH)$_2$X to produce the dihydride complexes [RuH$_2${(η^2-HSiR$_2$)$_2$X}(PCy$_3$)$_2$] (with R = Me and X = O (**2a**), C$_6$H$_4$ (**3**), (CH$_2$)$_2$ (**4**), (CH$_2$)$_3$ (**5**), OSiMe$_2$O (**6**)) and R = Ph, X = O (**2b**)). In these complexes, the bis(silane) ligand is coordinated to ruthenium via two σ-Si−H bonds, as shown by NMR, IR, and X-ray data and by theoretical calculations. **3**, **4**, and **6** were characterized by X-ray diffraction. In the free disilanes the Si−H bond distances and the $J_{\text{Si−H}}$ values are around 1.49 Å and 200 Hz, respectively, whereas in the new complexes the values are in the range 1.73−1.98 Å and 22−82 Hz, respectively for the σ-Si−H bonds. The importance of nonbonding H···Si interactions, which control the observed cis geometry of the two bulky PCy$_3$ ligands, is highlighted by X-ray data and theoretical calculations. The series of bis(silane) model complexes, RuH$_2${(η^2-HSiR$_2$)$_2$X}(PR′$_3$)$_2$, with X = (CH$_2$)$_2$, C$_6$H$_4$, (CH$_2$)$_n$, O, and OSiH$_2$O, and with R and R′ = H or Me, was investigated by density functional theory (DFT) by means of two hybrid functionals B3LYP and B3PW91. In the case of X = C$_6$H$_4$ three isomers were studied, the most stable of which has C_{2v} symmetry and whose structure closely resembles the X-ray structure of **3**. Calculated binding energies for the bis(silane) ligand to the RuH$_2$(PH$_3$)$_2$ fragment vary from 130 to 192 kJ/mol, showing that in the more stable complexes, the Si−H bonds are bound more strongly than dihydrogen. The dynamic behavior of these complexes has been studied by variable temperature ^{1}H and ^{31}P{^{1}H} NMR spectroscopy and exchange between the two types of hydrogen is characterized by barriers of 47.5 to 68.4 kJ/mol. The effect of the bridging group X between the 2 silicons is illustrated by reactions of compounds **2−6** with H$_2$, CO, ^{t}BuNC. **3** is by far the most stable complex as no reaction occurred even in the presence of CO, whereas elimination of the corresponding disilane and formation of RuH$_2$(H$_2$)$_2$-(PCy$_3$)$_2$, RuH$_2$(CO)$_2$(PCy$_3$)$_2$, or RuH$_2$(^{t}BuNC)$_2$(PCy$_3$)$_2$ were observed in the case of **2** and **4−6**. The mixed phosphine complexes [RuH$_2${(η^2-HSiMe$_2$)$_2$X}(PCy$_3$)(PR$_3$)] **3R−6R** (with R = Ph and R = pyl) have been isolated in good yields (80−85%) and fully characterized by the addition of 1 equiv of the desired phosphine to **3−6**. In the case of **4Ph**, an X-ray determination was obtained. In the case of **2**, elimination of the disiloxane was always observed. Addition of 1 equiv of a disilane to Ru(COD)(COT) in the presence of 2 equiv of the desired phosphine under an H$_2$ atmosphere produces the complexes [RuH$_2${(η^2-HSiMe$_2$)$_2$X}(PR$_3$)$_2$] (X = C$_6$H$_4$, R = Ph (**3Ph2**) and R = pyl (**3pyl2**); X = (CH$_2$)$_2$, R = Ph, **4Ph2**; R = pyl, **4pyl2**). **4Ph2** was also characterized by an X-ray structure determination.

Introduction

The first silane σ-complex was synthesized 30 years ago by Graham et al.,[1] thus years before the recognition of the agostic bond in 1983 [2] and the first publication of a dihydrogen complex.[3] Since that time, numerous examples of complexes bearing a σ Si−H bond have been reported.[4] Activation of Si−H bonds by metals is important in industrial processes such as hydrosilylation, dehydrogenative silylation, and polysilane production.[5] In these processes, σ-complexes are considered as intermediates in the key oxidative addition and reductive elimination steps (see Scheme 1 a). Therefore a better understanding of the factors that affect the stability and the nature of the silane addition products is highly desirable.

---

† Centre Nat. de la Recherche Scientifique.

‡ Université Paul Sabatier.

§ Permanent address: Department of Chemistry, Faculty of Sciences, University Al Baath, Homs, Syria.

(1) Hoyano, J. K.; Elder, M.; Graham, W. A. G. *J. Am. Chem. Soc.* **1969,** *91,* 4569.
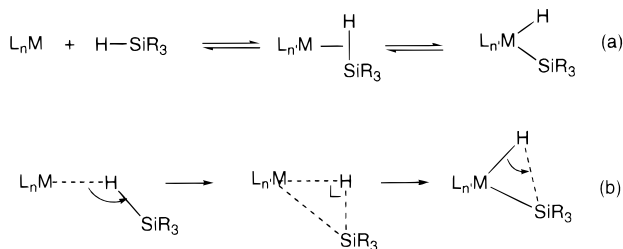
(2) Brookhart, M.; Green, M. L. H. *J. Organomet. Chem.* **1983,** *250,* 395.

(3) Kubas, G. J.; Ryan, R. R.; Swanson, B. I.; Vergamini, P. J.; Wasserman, H. J. *J. Am. Chem. Soc.* **1984,** *106,* 451.

(4) Schubert, U. *Adv. Organomet. Chem.* **1990,** *30,* 151.

---

(5) (a) Speier, J. L. *Adv. Organomet. Chem.* **1979,** *17,* 407. (b) Brown, S. S.; Kendrick, T. C.; McVie, J.; Thomas, D. R. In *Comprehensive Organometallic Chemistry*; Wilkinson, G., Stone, F. G. A., Abel, E. W., Eds.; Pergamon Press: New York, 1994; Vol. 2, Chapter 4. (c) West, R. In *The Chemistry of Organic Silicon Compounds*; Patai, S., Rappoport Z., Eds.; John Wiley & Sons: New York, 1989; Chapter 19. (d) Ojima, I. In *The Chemistry of Organic Silicon Compounds*; Patai, S., Rappoport, Z., Eds.; John Wiley & Sons: New York, 1989; Chapter 25. (e) Lapointe, A. M.; Rix, F. C.; Brookhart, M. *J. Am. Chem. Soc.* **1997,** *119,* 906. (f) Woo, H. G.; Waltzer, J. F.; Don Tilley, T. *J. Am. Chem. Soc.* **1992,** *114,* 7047. (g) Procopio, L. J.; Carroll, P. J.; Berry, D. H. *J. Am. Chem. Soc.* **1994,** *116,* 177.

Scheme 1

Scheme 2. Possible Structures Resulting from the Addition of Disilanes to Mononuclear Complexes

The most widely studied silane complexes are of the general formula $[(\eta^n\text{-}C_nR_n)(CO)LM(\eta^2\text{-}H\text{-}SiR'_3)]$ (M = Cr (n = 6), Mn (n = 5); L = CO, PR'$_3$; R = R' = alkyl, aryl), and their structures closely resemble those of oxidative addition products.[1,4,6,7] They are thus only slightly reactive and the stretched denomination, first applied for dihydrogen complexes,[8] can be used.

σ-(H−X) complexes result from a subtle balance between the σ donation from the H−X bond to an empty metal dσ orbital and the back-donation from the M(d) filled orbital of appropriate symmetry to the H−X σ^* orbital. Although this theoretical interpretation of the nature of the Si−H bonding has been recognized since the extended Hückel study of Rabaâ et al.[9] on CpMn(CO)$_2$(H···SiH$_3$) in 1987, it took about 10 years before a more sophisticated method was applied to the study of this type of complex. Recently, the nature of the M−H−Si triangular interactions has been investigated in the model complex Mo-(CO)(PH$_3$)$_4$(η^2-H−SiH$_3$) using MP2 perturbation theory by Fan et al.,[10a] and the same authors have analyzed theoretically the acceptor-capability of the Si−H σ^* orbital in titanium complexes.[10b] Maseras and Lledos have studied the relative stabilities of isomers of OsCl(CO)(PH$_3$)$_2$XY, where X and Y are either H and (η^2-H−SiH$_3$) or (η^2-H−H) and SiH$_3$ using MP4 energies at MP2 geometries.[10c]

We have synthesized in our group the two bis(dihydrogen) complexes RuH$_2$(H$_2$)$_2$(PCy$_3$)$_2$ (**1**) and Tp*RuH(H$_2$)$_2$ for which reactivity studies provide a good illustration of the bonding picture of the σ-H$_2$ bond.[11] In Tp*RuH(H$_2$)$_2$, modest back-bonding accounts for the electrophilic nature of the dihydrogen ligands, which is reflected by an absence of reactivity toward CH$_3$I or HBF$_4$ for example.[12] In contrast, **1** contains two labile dihydrogen ligands, allowing a versatile and rich reactivity that we have studied extensively.[13] In developing this theme, we have examined the reactivity of **1** toward weakly coordinating ligands, and we have been particularly interested in silane activation.[13d] We have shown in particular that **1** serves as a precursor for an efficient production of triethylvinylsilane resulting from dehydrogenative silylation of C$_2$H$_4$ by HSiEt$_3$.[14] We anticipated that extension of this system to functionalized silanes should be possible and we have recently reported the stoichiometric and catalytic activation of allyldimethylsilane.[15] In this context, disilane derivatives of the type HR$_2$SiXSiR$_2$H
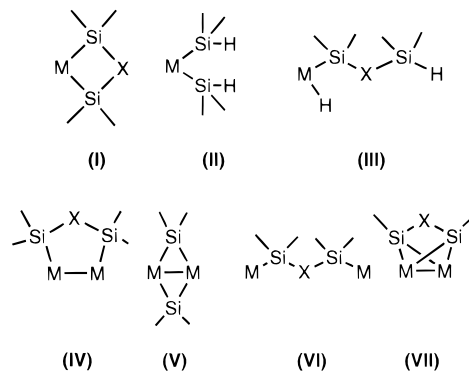
offer a unique opportunity to tune the properties of the resulting silicon compounds by changing the X bridge between the two silicons.

Addition of disilanes or disiloxanes HR$_2$SiXSiR$_2$H (X = O, C$_6$H$_4$, (CH$_2$)$_n$,...) to a mononuclear complex has so far only led to silyl complexes of the types shown in Scheme 2. When one to three atoms bridge the two silicons, structures of type I are generally observed. Thus, a wide family of chelating disilyl complexes have been obtained with several metals (Fe,[16] Ru,[16a] Os,[16a] Rh,[17] Ir,[17ab,18] Pd,[17a,19] Pt [20]). Four- or five-membered ring metallocycles are easily obtained but there are also some examples of six-membered ring metallocycles.[17a,20a] However, only one oxidative addition is observed by addition of HMe$_2$-Si(CH$_2$)$_4$SiMe$_2$H to Pt(PPh$_3$)$_2$(C$_2$H$_4$) producing the (hydrido)-silyl complex of type (III).[20a]

Before this work, no complex resulting from the coordination of a disilane compound with two σ Si−H bonds had been isolated. Complexes accommodating two σ bonds are rare: a few bis-agostic compounds are known,[21] and we have already mentioned the two thermally stable bis(dihydrogen) ruthenium complexes.[11] Recently bis or even tris β agostic Si−H yttrium

(6) Graham, W. A. G. *J. Organomet. Chem.* **1986**, *300*, 81.

(7) (a) Colomer, E.; Corriu, R. J. P.; Marzin, C.; Vioux, A. *Inorg. Chem.* **1982**, *21*, 368. (b) Carré, F.; Colomer, E.; Corriu, R. J. P.; Vioux, A. *Organometallics* **1984**, *3*, 1272.

(8) Crabtree, R. H. *Angew. Chem., Int. Ed. Engl.* **1993**, *32*, 789.

(9) Rabaâ, H.; Saillard, J. Y.; Schubert, U. *J. Organomet. Chem.* **1987**, *330*, 397.

(10) (a) Fan, M. F.; Jia, G.; Lin, Z. *J. Am. Chem. Soc.* **1996**, *118*, 9915. (b) Fan, M. F.; Lin, Z. *Organometallics* **1997**, *16*, 494. (c) Maseras, F.; Lledos, A. *Organometallics* **1996**, *15*, 1218.

(11) Sabo-Etienne, S.; Chaudret, B. *Coord. Chem. Rev.* **1998**, *178−180*, 381.

(12) Moreno, B.; Sabo-Etienne, S.; Chaudret, B.; Rodriguez, A.; Jalon, F.; Trofimenko, S. *J. Am. Chem. Soc.* **1995**, *117*, 7441.

(13) See, for example: (a) Arliguie, T.; Chaudret, B.; Morris, R. H.; Sella, A. *Inorg. Chem.* **1988**, *27*, 598. (b) Chaudret, B.; Chung, G.; Eisenstein, O.; Jackson, S. A.; Lahoz, F.; Lopez, J. A. *J. Am. Chem. Soc.* **1991**, *113*, 2314. (c) Christ, M. L.; Sabo-Etienne, S.; Chaudret, B. *Organometallics* **1994**, *13*, 3800. (d) Sabo-Etienne, S.; Hernandez, M.; Chung, G.; Chaudret, B.; Castel, A. *New J. Chem.* **1994**, *18*, 175. (e) Borowski A.; Sabo-Etienne, S.; Christ, M. L.; Donnadieu B.; Chaudret, B. *Organometallics* **1996**, *15*, 1427. (f) Guari, Y.; Sabo-Etienne, S.; Chaudret, B. *Organometallics* **1996**, *15*, 3471. (g) Guari, Y.; Sabo-Etienne, S.; Chaudret, B. *J. Am. Chem. Soc.* **1998**, *120*, 4228. (h) Rodriguez, V.; Sabo-Etienne, S.; Chaudret, B.; Thoburn, J.; Ulrich, S.; Limbach, H. H.; Eckert, J.; Barthelat, J. C.; Hussein, K.; Marsden, C. J. *Inorg. Chem.* **1998**, *37*, 3475.

(14) Christ, M. L.; Sabo-Etienne, S.; Chaudret, B. *Organometallics* **1995**, *14*, 1082.

(15) Delpech, F.; Sabo-Etienne, S.; Donnadieu, B.; Chaudret, B. *Organometallics* **1998**, *17*, 4926.

(16) (a) Vancea, L.; Graham, W. A. G. *Inorg. Chem.* **1974**, *3*, 511. (b) Corriu, R. J. P.; Moreau, J. J. E.; Pataud-Sat, M. *J. Organomet. Chem.* **1982**, *228*, 301. (c) Corriu, R. J. P.; Moreau, J. J. E.; Pataud-Sat, M. *Organometallics* **1985**, *4*, 623.

(17) (a) Curtis, M. D.; Greene, J. *J. Am. Chem. Soc.* **1978**, *100*, 6362. (b) Curtis, M. D.; Epstein, P. S. *Adv. Organomet. Chem.* **1981**, *19*, 213. (c) Osakada, K.; Hataya, K.; Nakamura, Y.; Tanaka, M.; Yamamoto, T *J. Chem. Soc., Chem. Commun.* **1993**, 576. (d) Nagashima, H.; Tatebe, K.; Ishibashi, T.; Nakaoka, A.; Sakakibara, J.; Itoh, K. *Organometallics* **1995**, *14*, 2868.

(18) Loza, M.; Faller, J. W.; Crabtree, R. H. *Inorg. Chem.* **1995**, *34*, 2937.

(19) Shimada, S.; Tanaka, M.; Shiro, M. *Angew. Chem., Int. Ed. Engl.* **1996**, *35*, 1856.

(20) (a) Eaborn, C.; Metham, T. N.; Pidcock, A. *J. Organomet. Chem.* **1973**, *63*, 107. (b) Shimada, S.; Tanaka, M.; Honda, K. *J. Am. Chem. Soc.* **1995**, *117*, 8289. (c) Lemanski, M. F.; Schram, E. P. *Inorg. Chem.* **1976**, *15*, 1489. (d) Schubert, U.; Müller, C. *J. Organomet. Chem.* **1991**, *418*, C6.

Table 1. Selected NMR Data for [RuH$_2${(η^2-HSiR$_2$)$_2$X}(PCy$_3$)$_2$], **2**−**6**

X	complexes	δ_{SiMe}	δ_{SiH}	δ_{RuH}	$\Delta G^{\ddagger}$ (kJ/mol)	T_c (K)	δ_P	δ_{Si}	J_{SiP} (Hz)	J_{SiH} (Hz)
			¹H NMR[a,b]				³¹P NMR,[a,c]	²⁹Si NMR[a,d]		
O	**2a**	1.12	−9.48		47.5	253	49.9	−5.61		22
O	**2b**		−8.60		51.0	273	45.4	4.80		41
C$_6$H$_4$	**3**	1.16	−7.74	−12.03	64.5	357	51.0	4.77	8.3	65
(CH$_2$)$_2$	**4**	0.93	−8.21	−12.65	68.4	376	50.9	12.20	7.6	70
(CH$_2$)$_3$	**5**	0.87	−8.49	−12.17	62.5	343	51.0	−11.14	5.3	75
OSiMe$_2$O	**6**	1.06	−9.14	−11.20	62.5	333	49.8	4.91	9.2	82

[a] C$_6$D$_6$, 288 K. [b] 400 MHz. [c] 161.99 MHz. [d] 79.5 MHz.

Table 2. Crystal data for RuH$_2${(η^2-HSiMe$_2$)$_2$C$_6$H$_4$}(PCy$_3$)$_2$,C$_6$H$_6$ (**3**), RuH$_2${(η^2-HSiMe$_2$)$_2$(CH$_2$)$_2$}(PCy$_3$)$_2$ (**4**), RuH$_2${(η^2-HSiMe$_2$)$_2$(CH$_2$)$_2$}(PCy$_3$)(PPh$_3$), (C$_6$H$_6$)$_2$ (**4Ph**), RuH$_2${(η^2-HSiMe$_2$)$_2$(CH$_2$)$_2$}(PPh$_3$)$_2$ (**4Ph$_2$**), and RuH$_2${(η^2-HSiMe$_2$)$_2$OSiMe$_2$O}(PCy$_3$)$_2$, [(C$_2$H$_5$)$_2$O]$_{0.5}$ (**6**)

	3	4	4Ph	4Ph$_2$	6
formula	C$_{44}$H$_{88}$P$_2$Si$_2$Ru, C$_6$H$_6$	C$_{42}$H$_{86}$P$_2$Si$_2$Ru	C$_{42}$H$_{68}$P$_2$Si$_2$Ru, (C$_6$H$_6$)$_2$	C$_{42}$H$_{50}$P$_2$Si$_2$Ru	C$_{42}$H$_{88}$O$_2$P$_2$Si$_3$Ru, (C$_2$H$_5$OC$_2$H$_5$)$_{0.5}$
fw(g)	936.49	810.34	948.42	774.05	909.50
color	colorless	colorless	colorless	colorless	yellow
crystal system	monoclinic	monoclinic	triclinic	monoclinic	monoclinic
space group	$I2/a$	Cc	$P\bar{1}$	$P2_1/c$	$C2/c$
temp, K	180	160	180	150	180
a, Å	20.894(2)	12.719(2)	9.908(1)	18.072(3)	20.272(2)
b, Å	19.520(2)	19.109(2)	10.929(1)	10.781(1)	19.862(3)
c, Å	25.113(2)	18.068(2)	24.783(2)	20.773(3)	24.910(3)
α, deg	90.0	90.0	99.04(1)	90.0	90.0
β, deg	90.33(1)	90.59(1)	99.50(1)	106.86(2)	93.94(1)
γ, deg	90.0	90.0	100.30(1)	90.0	90.0
V, Å^3	10242(1)	4391.0(8)	2555.6(8)	3873(1)	10006(2)
Z	8	4	2	4	8
R	0.0257	0.0215	0.0318	0.0268	0.0326
R_w	0.0313	0.0244	0.0355	0.0278	0.0400
GOF	0.968	1.017	1.078	1.064	1.095

or erbium complexes have been isolated.[22] There are several dinuclear complexes in which two Si−H bonds are η^2-coordinated but with only one η^2-Si−H bond on each metal center.[23] There is however a series of compounds {[Cp*Ru]$_2$-(μ-η^2-HSiRR′)(μ-η^2-HSiR″R‴)(μ-H)(H)} in which the two β agostic interactions are on the same metal center.[24,25] In 1989, Luo and Crabtree described the reaction of 2 equiv of Et$_3$SiH or HEt$_2$SiSiEt$_2$H with [IrH$_2$(THF)$_2$(PPh$_3$)$_2$](SbF$_6$): they identified two mononuclear complexes by ¹H NMR for which they proposed the coordination of two σ Si−H bonds.[26]

We reasoned that **1** with its two labile dihydrogen ligands was an ideal candidate to study the activation of disilanes and disiloxanes. We wish to report here the synthesis of the first examples of fully characterized transition metal bis(silane) complexes [RuH$_2${(η^2-HSiMe$_2$)$_2$X}(PCy$_3$)$_2$], in which two H−Si bonds are η^2-coordinated to the same metal. Extensive spectroscopic and structural characterizations, as well as theoretical

calculations, allow a detailed description of the bonding mode of the chelating bis(silane) ligand, and highlight the importance of formally nonbonding H···Si interactions. The influence of the bridge between the two silicon atoms is also illustrated by simple reactivity studies. Our results concerning the catalytic activation of dihydrogenosilanes (or siloxanes) will be described in a future paper. A preliminary account of part of this work has appeared.[27]

Results

A. Synthesis and Spectroscopic Properties of the Bis-(silane) Complexes [RuH$_2${(η^2-HSiMe$_2$)$_2$X}(PCy$_3$)$_2$] (with X = O (2a), C$_6$H$_4$ (3), (CH$_2$)$_2$ (4), (CH$_2$)$_3$ (5), OSiMe$_2$O (6)), and [RuH$_2${(η^2-HSiPh$_2$)$_2$O}(PCy$_3$)$_2$] (2b). Reaction of RuH$_2$-(H$_2$)$_2$(PCy$_3$)$_2$ (**1**) with 1 equiv or more of bis(silane) compounds HR$_2$SiXSiR$_2$H was carried out in pentane at room temperature. The reaction proceeded rapidly with gas evolution and after workup, white powders were isolated in high yield (72−94%) and analyzed as [RuH$_2${(η^2-HSiR$_2$)$_2$X}(PCy$_3$)$_2$] (with R = Me and X = O (**2a**), C$_6$H$_4$ (**3**), (CH$_2$)$_2$ (**4**), (CH$_2$)$_3$ (**5**), OSiMe$_2$O (**6**)), and R = Ph, X = O (**2b**)). The complexes are characterized by multinuclear NMR (see Table 1) and IR spectroscopies (see Table 7) and by single-crystal X-ray diffraction in the case of **3**, **4**, and **6** (see Tables 2−4, 6 and Figures 3, 4). They result from the substitution of the two dihydrogen ligands of **1** by the corresponding disilane (see Scheme 3). The coordination of the bis(silane) ligand to the metal center via two (η^2-Si−H) bonds is demonstrated by ²⁹Si NMR and IR data and confirmed by X-ray determination in three cases. All of the complexes give a single line in the range δ 45−51 in the ³¹P{¹H} NMR spectra at room temperature, indicative of two equivalent phosphine ligands.

(21) (a) King, W. A.; Luo, X.-L.; Scott, B. L.; Kubas, G. J.; Zilm, K. W. *J. Am. Chem. Soc.* **1996**, *118*, 6782. (b) Poole, A. D.; Williams, D. N.; Kenwright, A. M.; Gibson, V. C.; Clegg, W.; Hockless, D. C. R.; O'Neil, P. A. *Organometallics* **1993**, *12*, 2549 and references therein.

(22) (a) Herrmann, W. A.; Munck, F. C.; Artus, G. R. J.; Runte, O.; Anwander, R. *Organometallics* **1997**, *16*, 682. (b) Herrmann, W. A.; Eppinger, J.; Spiegler, M.; Runte, O.; Anwander, R. *Organometallics* **1997**, *16*, 1813. (c) Rees, W. S.; Just, O.; Schumann, H.; Weimann, R. *Angew. Chem., Int. Ed. Engl.* **1996**, *35*, 419.

(23) (a) Butts, M. D.; Bryan, J. C.; Luo, X. L.; Kubas, G. J. *Inorg. Chem.* **1997**, *36*, 3341. (b) Fryzuk, M. D.; Rosenberg, L.; Rettig, S. J. *Inorg. Chim. Acta* **1994**, *222*, 345. (c) Dioumaev, V. K.; Harrod, J. F. *Organometallics* **1996**, *15*, 3859. (d) Simons, R. S.; Tessier, C. A. *Organometallics* **1996**, *15*, 2604. (e) Kim, Y. J.; Lee, S. C.; Park, J. I.; Osakada, K.; Choi, J. C.; Yamamoto, T. *Organometallics* **1998**, *17*, 4929.
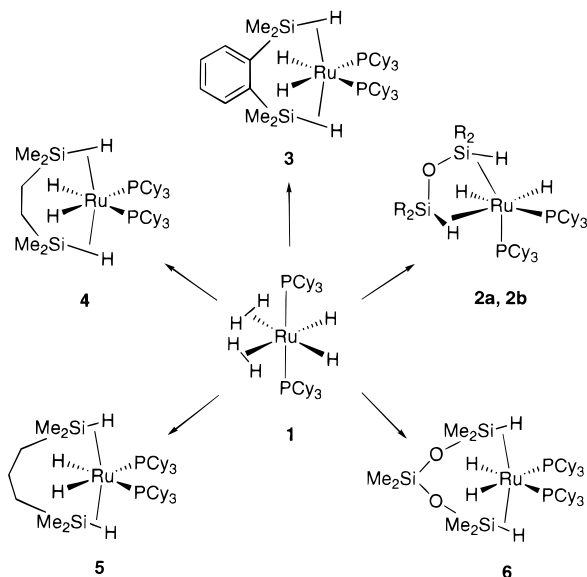
(24) (a) Takao, T.; Yoshida, S.; Suzuki, H.; Tanaka, M. *Organometallics* **1995**, *14*, 3855. (b) Suzuki, H.; Takao, T.; Tanaka, M.; Moro-oka, Y. *J. Chem. Soc., Chem. Commun.* **1992**, 476.

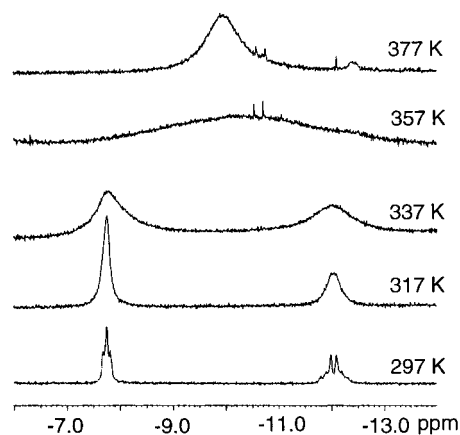(25) Campion, B. K.; Heyn, R. H.; Don Tilley, T. *Organometallics* **1992**, *11*, 3918.

(26) Luo, X. L.; Crabtree, R. H. *J. Am. Chem. Soc.* **1989**, *111*, 2527.

(27) Delpech, F.; Sabo-Etienne, S.; Chaudret, B.; Daran, J. C. *J. Am. Chem. Soc* **1997**, *119*, 3167.

Table 3. Selected Interatomic Distances (Å) and Angles (deg) for the Bis(silane) Complexes **4**, **4Ph**, **4Ph₂**

	4	4Ph	4Ph₂
Ru−Hb1	1.55(3)	1.64(3)	1.63(3)
Ru−Hb2	1.54(3)	1.66(3)	1.59(3)
Si1−Hb1	1.73(3)	1.80(3)	1.93(3)
Si2−Hb2	1.78(3)	1.98(3)	1.87(3)
Ru−H1	1.53(3)	1.65(3)	1.54(3)
Ru−H2	1.60(3)	1.49(3)	1.59(3)
Ru1−Si1	2.4282(6)	2.4623(7)	2.4481(7)
Ru1−Si2	2.4109(7)	2.4214(7)	2.4326(7)
Ru1−P1	2.4474(6)	2.4219(7)	2.3694(7)
Ru1−P2	2.4244(6)	2.3777(7)	2.3621(7)
Ru1−Hb1−Si1	95.1(14)	91.4(15)	86.2(14)
Ru1−Hb2−Si2	92.9(13)	82.9(14)	89.1(15)
Hb1−Ru−Hb2	176.3(17)	172.3(15)	171.1(15)
Si1−Ru−Si2	87.36(3)	86.33(3)	86.67(2)
H1−Ru−H2	102.5(12)	100.3(17)	99.1(16)
P1−Ru−P2	108.243(17)	105.06(2)	104.22(2)
P1−Ru−H1	175.9(11)	173.2(11)	177.2(11)
P2−Ru−H2	175.1(10)	172.6(12)	177.5(11)

Scheme 3. Synthesis of **2**−**6** by Addition of the Corresponding Disilane to **1**

**Figure 1.** 250 MHz ¹H NMR spectra of **3** in C₇D₈ at various temperatures.

The ¹H NMR spectra of **2**−**6** are temperature-dependent. In the case of **3**−**6**, coalescence of the two signals in the hydride region is obtained at high temperature, leading to one broad signal (see Figure 1). The exchange between the (η²-Si−H) and Ru−H hydrides is characterized by a barrier of 64.5 kJ/mol for **3**, 68.4 kJ/mol for **4**, 62.5 kJ/mol for **5**, and 62.5 kJ/mol for **6** (uncertainties of the order of 0.8 kJ/mol). These values are significantly higher than those measured for **2a,b**: decoalescence is observed at 253 and 273 K, respectively, leading to two broad triplets at δ −8.5 ($J_{\text{H−P}}$ 13 Hz) and −9.9 ($J_{\text{H−P}}$ 45 Hz) for **2a**, and a broad singlet at δ −7.6 together with a broad triplet at δ −9.36 ($J_{\text{H−P}}$ 43 Hz) for **2b**. These processes are characterized by a $\Delta G^{\ddagger}$ of 47.5 and 51 kJ/mol, respectively. In the case of **2a**, a second decoalescence is achieved on cooling further. The slow exchange limit is obtained at 178 K, and four broad signals of equal intensity are observed at δ −8.1, −8.5, −9.4, and −10.2. The two coalescence temperatures at 198 and 190 K combined with the $\Delta \nu$ = 195 and 94.5 Hz, respectively for the two types of protons give a $\Delta G^{\ddagger}$ of roughly 38 kJ/mol. The ³¹P{¹H} spectrum shows two very broad signals at 178 K, at δ 53.2 and 52.7, with a $J_{\text{P−P}}$ value of 27.5 Hz in agreement with a cis disposition of the two phosphines, indicative of an arrested structure.

A labeling experiment gives further information about the exchange process. The deuterated compound DSiMe₂(CH₂)₃-SiMe₂D was obtained by reaction of LiAlD₄ with ClSiMe₂(CH₂)₃-SiMe₂Cl. Full deuteration was indicated by the total disappearance of the Si−H septet at δ 4.25 and the shift of the $\nu_{\text{Si−H}}$ band from 2113 to 1537 cm⁻¹ in the deuterated isomer. Addition to **1** resulted in the formation of the d^2 isotopomer **5-d** which we have isolated and characterized by NMR and IR spectroscopies. The ¹H NMR spectrum still shows the two resonances in a 1:1 integration ratio in the hydride region, but integration of these two signals against those at low field and particularly the methyl protons bound to the silicons at δ 0.87 indicates 50% deuterium incorporation in each hydride site. Deuterium incorporation into the classical hydride sites implies a rather easy exchange process between the hydrides and the (η²-Si−H) protons. Deuterium incorporation in these two groups is confirmed by ²H{¹H,³¹P} NMR: two broad signals are observed at δ −8.5 and δ −12.2. The broad signal observed in the ³¹P{¹H} NMR spectrum at δ 51.2 does not allow us to distinguish the different isomers, but the signal is clearly distorted on the high-field side, indicating a very small isotopic shift. In addition, a spin saturation transfer experiment shows a 50% decrease in the intensity of the signal at δ −12.2 when irradiating the multiplet at δ −8.5, and vice versa.

The ¹H NMR spectra of **3**−**6** exhibit two resonances in the hydride region at room temperature, in a 1:1 integration ratio. The triplet near δ −8 is attributed to the two η²- bound Si−H protons, whereas the AA′XX′ multiplet near δ −12 is attributed to the two classical hydrides. The reduced $J_{\text{H−P}}$ value of 13 Hz within the triplet can be compared to $J_{\text{H−P}}$ values generally observed for dihydrogen complexes (<5 Hz)[28,11] and suggests stretching of the Si−H bonds. Upon phosphorus decoupling, both resonances appear as a singlet. In contrast, complexes **2a,b** show only one broad line in the hydride region at room temperature, near δ −9. The absence of any (η²- H₂) ligand in all of the new complexes was confirmed by T_1 measurements: $T_{1\text{min}}$ values higher than 140 ms were obtained. In the case of R = Me, all of the complexes **2a**, **3**−**6** give a single line at room temperature, near δ 1 integrating for 12H for the methyl groups bound to silicon. Thus, upon coordination, the methyl protons are clearly deshielded (they are observed between δ 0.15 to 0.32 in the free disilanes). In the case of **6**, another singlet integrating for 6H is observed at δ 0.55 for the two methyl groups bound to the inner silicon not coordinated to the ruthenium.

(28) Jessop, P. G.; Morris, R. H. *Coord. Chem. Rev.* **1992**, *121*, 155.

Table 4.   Calculated Geometrical Parameters[a] for the RuH$_2$((η^2-HSiH$_2$)$_2$X)(PH$_3$)$_2$ Ground State and X-ray Data for **3** and **4**
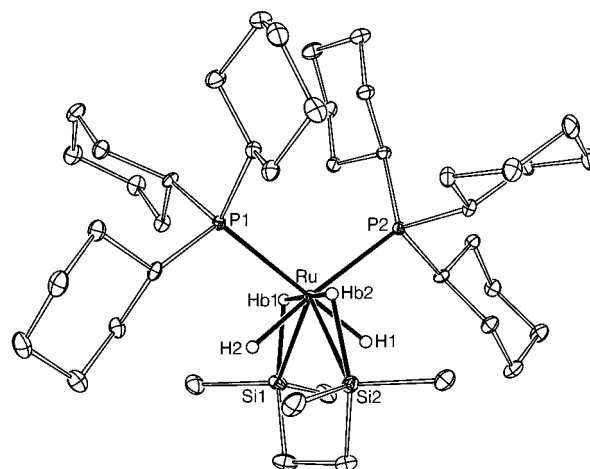
X	C$_6$H$_4$			CH$_2$	(CH$_2$)$_2$		(CH$_2$)$_3$	(CH$_2$)$_4$
	B3LYP	B3PW91	X-ray for **3** (180 K)	B3LYP	B3LYP	X-ray for **4** (160 K)	B3LYP	B3LYP
Ru−Hb1(2)	1.681	1.672	1.60(3), 1.59(3)	1.663, 1.807	1.683	1.55(3), 1.54(3)	1.674	1.664
Si1(2)−Hb1(2)	1.848	1.867	1.84(2), 1.84(2)	1.768, 1.585	1.853	1.73(3), 1.78(4)	1.880	1.866
Si1(2)···H1(2)	2.253	2.236	2.22(2), 2.21(2)	2.867, 2.708	2.220	2.27(3), 2.31(3)	2.170	2.151
Si1(2)···H2(1)	2.253	2.236	2.18(2), 2.12(2)	2.139, 4.231	2.329	2.13(3), 2.12(3)	2.450	2.576
Ru−Si1(2)	2.425	2.409	2.4162(5), 2.4280(5)	2.464, 2.735	2.441	2.4282(6), 2.4109(7)	2.447	2.466
Ru−H1(2)	1.632	1.632	1.59(3), 1.54(2)	1.613, 1.631	1.631	1.53(3), 1.60(3)	1.620	1.628
Ru−P1(2)	2.378	2.345	2.4628(4), 2.4537(4)	2.371, 2.334	2.376	2.4474(6), 2.4244(6)	2.384	2.381
Ru−Hb1(2)−Si1(2)	86.7	85.6	88.7(11), 90.1(12)	91.7, 107.3	87.2	95.1(14), 92.9(13)	85.8	88.4
Hb1−Ru−Hb2	172.4	170.6	172.9(12)	92.1	173.7	176.3(17)	170.6	166.5
Hb1(2)−Ru−H1(2)	92.3	92.9	91.9(12), 90.6(12)	104.5, 173.8	94.0	87.7(15), 87.2(14)	99.9	104.6
Hb2(1)−Ru−H1(2)	92.3	92.9	94.5(12), 91.6(12)	102.3, 87.4	89.8	94.4(15), 89.3(15)	85.8	84.3
Si1−Ru−Si2	88.5	88.2	87.943(17)	70.0	88.3	87.36(3)	94.0	107.4
H1−Ru−H2	104.5	104.3	98.8(11)	83.8	105.9	102.5(12)	105.9	98.7
P1(2)−Ru−H1(2)	177.0	177.3	175.2(8), 171.8(8)	167.6, 85.2	175.5	175.9(11), 175.1(10)	172.3	171.7
P1(2)−Ru−H2(1)	78.5	78.4	78.8 (8), 73.8 (8)	84.7, 78.6	78.1	76.4(10), 72.9(10)	78.3	82.2
P1(2)−Ru−Si1(2)	117.9	117.8	117.75(2), 120.12(2)	124.9, 101.7	114.6	116.80(2), 111.52(2)	106.7	98.8
P1(2)−Ru−Si2(1)	117.9	117.8	112.30(2), 109.12(2)	120.5, 137.3	121.7	115.86(2), 115.99(2)	127.2	128.6
P1−Ru−P2	98.4	98.9	108.80(2)	95.9	98.0	108.243(17)	98.2	98.2

[a] See Figures 5 and 6 for labeling of the atoms. Distances are in Å and angles in degrees.
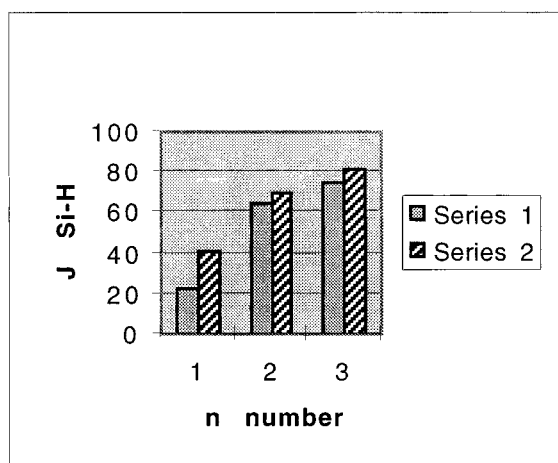
Figure 2. Plot of $J_{Si−H}$ values (Hz) vs the number (n) of atoms bridging the two silicons within the bis(silane) complexes **2**−**6**. Series 1 with n = 1, **2a**; n = 2, **3**; n = 3, **5**. Series 2 with n = 1, **2b**; n = 2, **4**; n = 3, **6**.

Figure 3. ORTEP view of compound **4**. Ellipsoids are drawn at 50% probability level.

Various ^{29}Si NMR experiments were performed in order to determine the $J_{Si−P}$ and $J_{Si−H}$ values. Data are reported in Table 1. The values of $\delta(^{29}Si)$ for the different compounds vary in a relatively narrow range: from δ 12.2 to 11.1. The ^{29}Si {^{1}H} NMR spectra for **3**−**6** show a triplet with a $J_{Si−P}$ value close to 8 Hz and the ^{29}Si {^{31}P} INEPT spectra show a doublet with $J_{Si−H}$ values between 22 and 82 Hz. The magnitude of $J_{Si−H}$ can be related to the length of the bridge between the two silicons: the lowest values are obtained for **2a,b** (22 and 41 Hz, respectively) in which only one atom connects the two silicons; intermediate values are found for compounds **3** and **4** (65 and 70 Hz, respectively), and the highest values are obtained for **5** and **6** in which three atoms connect the two silicons (75 and 82 Hz, respectively) (see Figure 2). The data can be rationalized as follows: (i) All of the values fall in the range corresponding to a M-(η^2-Si−H) interaction; in no case does the activation of the disilane result in the breaking of the Si−H bonds, and no hydrido(silyl) complex is obtained. (ii) The degree of activation of the Si−H bonds is to a certain extent related to the chain length between the two silicons: a weak activation is favored by a long chain, as reflected by the values observed for compounds **5** and **6**.

The IR spectra (in Nujol) of compounds **2**−**6** display two broad bands for the Ru−H stretches in the range 2045−1955 cm^{-1} characteristic of a cis dihydride structure and an intense broad band for the Ru−(η^2-Si−H) bonds in the range 1670−1800 cm^{-1} (see Table 7). The ν (H−Si) of the free disilane is found at 2111 cm^{-1} for (HSiMe$_2$)$_2$(CH$_2$)$_2$, 2113 cm^{-1} for (HSiMe$_2$)$_2$(CH$_2$)$_3$, 2122 cm^{-1} for (HSiPh$_2$)$_2$O, 2129 cm^{-1} for (HSiMe$_2$)$_2$O and for (HSiMe$_2$)$_2$(OSiMe$_2$O), and 2148 cm^{-1} for (HSiMe$_2$)$_2$(C$_6$H$_4$). Thus, a low-frequency shift of 310 cm^{-1} in the case of **5** and up to 452 cm^{-1} in the case of **2b** is observed for the activated Ru−(η^2-Si−H) bonds. Further analysis will be found in the theoretical section. Complexation of the disilane also results in a splitting of the band of the SiMe$_2$ groups into 2 or 3 bands between 1230 and 1270 cm^{-1}. In the bis-(dihydrogen) complex **1**, two Ru−H stretches are observed at 1927 and 1890 cm^{-1}. These bands cannot be considered as pure modes (coupling with the (η^2- H$_2$) ligands must be present),[29] but they are clearly shifted to low frequencies by comparison to the bands observed for all the bis(silane) complexes **2**−**6**.

B. X-ray Structural Determination of [RuH$_2${(η^2-HSi-Me$_2$)$_2$X}(PCy$_3$)$_2$] (with X = C$_6$H$_4$ (3), (CH$_2$)$_2$ (4), OSiMe$_2$O (6)). The X-ray structures of **3**, **4**, and **6** were determined at
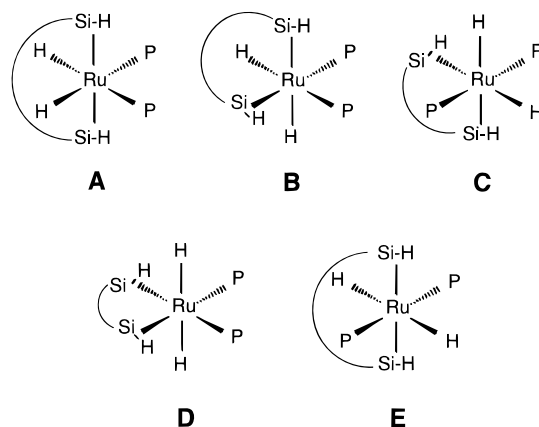
(29) Bender, B. R.; Kubas, G. J.; Jones, L. H.; Swanson, B. I.; Eckert, J.; Capps, K. A.; Hoff C. D. *J. Am. Chem. Soc.* **1997**, *119*, 9179.
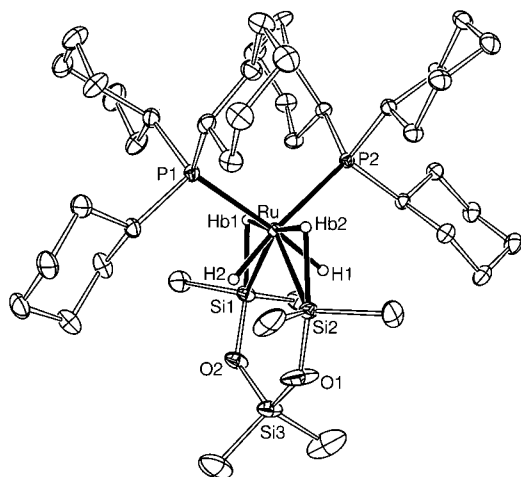
Figure 4. ORTEP view of compound **6**. Ellipsoids are drawn at 50% probability level.

low temperature (see Tables 2, 3, 4, and 6 and Figures 3 and 4). The X-ray structure of **3** has already been reported in the preliminary paper but at room temperature.[27] Low-temperature measurements allow better location of the hydrogen atoms. The three compounds present roughly the same geometry. The ruthenium atom is in a pseudo-octahedral environment. The chelating bis(silane) occupies two coordination sites with the hydrogens being in the axial positions. The angles Hb1−Ru−Hb2 are greater than 170°. The phosphines are in a cis position and the P−Ru−P angle remains the same for the 3 structures (∼108°). A trans geometry for the two tricyclohexylphosphines is generally observed in [Ru](PCy₃)₂ complexes.[11] In our compounds a cis position results from the stabilization of the disilane coordination through an interaction between the terminal hydrides H1 and H2 and the Si atoms (see Theoretical Calculations and Discussion). We will see in the Reactivity Studies that for phosphines with different steric and electronic properties the same geometry is obtained. The plane containing the ruthenium, the two phosphorus atoms, and the two hydrides is perpendicular to that containing the two (η²-Si−H) ligands. The (η²-Si−H) coordination is confirmed by a significant lengthening of the Si−Hb bonds: 1.84(2) Å for **3**, 1.73(3) and 1.78(3) Å for **4**, and 1.81(3) and 1.77(4) Å for **6** (∼1.49 Å in the free disilanes). The four Ru−H bond lengths are undifferentiated (∼1.6 Å) for the three compounds and similar to those normally observed for ruthenium hydride complexes. The nonbonding Si···H distances vary from 2.04 to 2.43 Å, thus allowing some Si···H interaction as we will see in the Discussion. The Ru−Hb−Si angles are close to 90° for the three compounds. The Ru−Si distance is also a good indicator of the degree of activation of the Si−H bond. η²-Silane complexes normally have Si−H distances higher than silyl complexes. In mononuclear silyl ruthenium complexes, the Ru−Si distances are in the range 2.34−2.45 Å.[30] In our compounds, the Ru−Si bond lengths vary from 2.41 to 2.48 Å, thus comparatively longer. The Si−Ru−Si angles in **3** (87.94(2)°) and **4** (87.36-(3)°) are similar. Thus the rigidity due to the ring in **3** has no influence on the structure, whereas in **6**, a longer chain between the two silicons imposes a more open angle (97.25(2)°). It is noteworthy that in our bis(silane) compounds the two (η²-Si−H) bonds impose an opening of the Si−M−Si angle by comparison to disilylmetallocles. For example, the Si−M−Si angle in the six-membered ring metallocycle [Pd][SiMe₂(CH₂)₃-

(30) Don Tilley, T. In *The Silicon-Heteroatom Bond*; Patai, S., Rappoport, Z., Eds.; John Wiley & Sons: Chichester, 1994; Chapter 9.

Scheme 4. Five Possible Isomers for the Bis(silane) Complexes

SiMe₂] is 85.8°,[31] whereas in the five-membered ring [Rh]-[SiMe₂(CH₂)₂SiMe₂][17c] it is reduced to 80.5° and 80.7° in [Ir][SiMe₂(C₆H₄)SiMe₂].[18] It should be noted that in this last example, an addition reaction of HSiMe₂(C₆H₄)SiMe₂H to IrH₅-(PPh₃)₂ is observed, affording the trihydride bis(silyl) iridium complex IrH₃[SiMe₂(C₆H₄)SiMe₂](PPh₃)₂ with loss of dihydrogen, as opposed to the substitution of H₂ by the disilane observed during the formation of **3**.

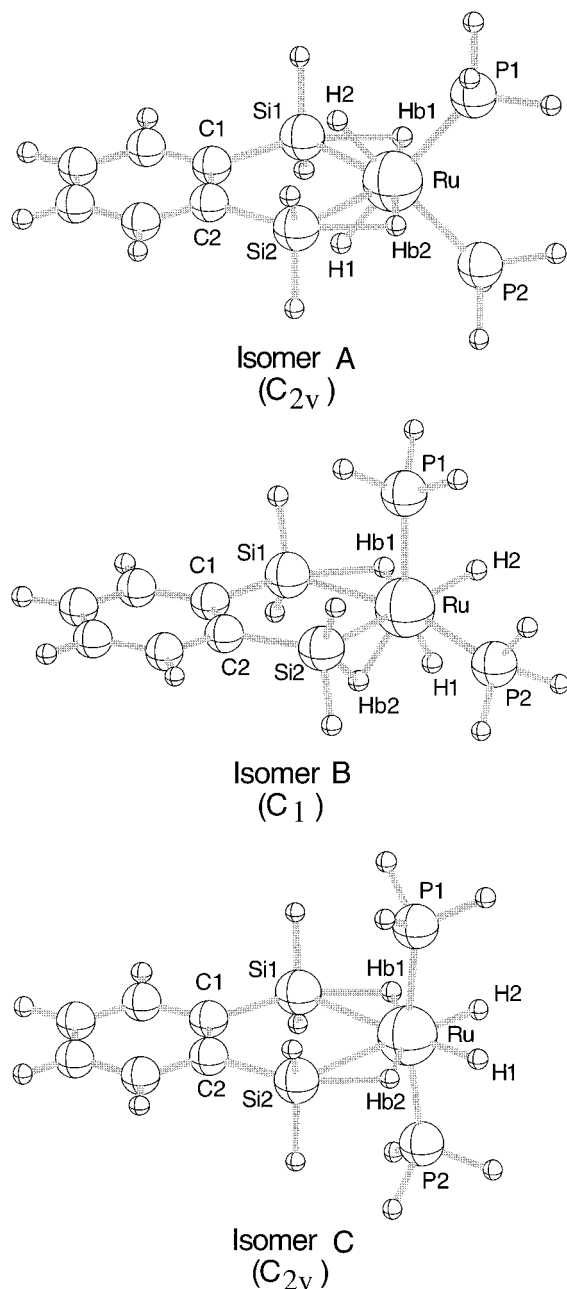**C. Theoretical Calculations.** A series of chelating bis(silane) model complexes, RuH₂{(η²-HSiR₂)₂X}(PR′₃)₂, with X = (CH)₂, C₆H₄, (CH₂)ₙ, O, and OSiH₂O and with R and R′ = H or Me, was investigated in order to understand the coordination of the Si−H σ bond to the ruthenium center. Five isomers can be envisaged for the complexes in which X = C₆H₄ or (CH)₂ and R = R′ = H, depending on the relative orientations of the various ligands. All five may be described as pseudo-octahedral with two cis or trans phosphines (see Scheme 4, where P represents PR′₃). The isomers that contain two mutually trans hydrides, D and E, need not be considered in detail. They would be very high-energy structures due to the strong σ-donor ability of the hydride ligand.[32] The three other isomers (A, B, and C) have been characterized on the singlet potential energy surface. They are depicted in Figure 5 where X = C₆H₄; optimized geometrical parameters for isomer A, obtained from two different hybrid functionals B3LYP and B3PW91, are summarized in Table 4. Selected distances calculated for the three isomers A, B, and C (X is C₆H₄) at the B3LYP level of theory are presented in Table 5. Vibrational frequency calculations showed all three isomers to be local minima. It was important to determine whether the structural and energetic comparisons studied here are sensitive to the particular variety of DFT employed. A detailed comparison of the B3LYP and B3PW91 geometrical results in Table 4 shows only trivial differences between the two sets; the relative energies found with the two computational methods for isomers A, B, and C for the complex where X is CH=CH are also very similar.

The geometry of isomer A is a C_{2v} distorted octahedron in which the two axial coordination sites are occupied by the η²-Si−H bonds of the chelating bis(silane) ligand. The structure of this isomer closely resembles that found by low-temperature X-ray diffraction for **3** in all important respects. The two H atoms from the η²-Si−H bonds, denoted Hb, are therefore almost trans to each other. They occupy bridging positions between a Si and the Ru, giving an Hb1−Ru−Hb2 angle of

(31) Suginome, M.; Oike, H.; Shuff, P. H.; Ito, Y. *Organometallics* **1996**, *15*, 2170.

(32) Clot, E.; Eisenstein, O. *J. Phys. Chem.* **1998**, *102*, 3592.

Figure 5. The three B3LYP-optimized isomeric structures of RuH$_2$-{(η^2-HbSiH$_2$)$_2$C$_6$H$_4$}(PH$_3$)$_2$.

Table 5. Selected Ruthenium−Hydrogen and Silicon−Hydrogen Distances (in Å) for the Three Isomers of RuH$_2$((η^2-HSiH$_2$)$_2$C$_6$H$_4$)(PH$_3$)$_2$ Calculated at the DFT/B3LYP Level of Theory

isomer	A	B[a]	C
Ru−Hb1	1.681	1.629	1.662
Ru−Hb2	1.681	1.621	1.662
Ru−H1	1.632	1.606	1.623
Ru−H2	1.632	1.644	1.623
Si1−Hb1	1.848	1.808	1.715
Si1···H2	2.253	3.521	3.423
Si2−Hb2	1.848	2.144	1.715
Si2···H1	2.253	3.582	3.423

[a] For the nonsymmetrical isomer B, there are two other significant silicon−hydrogen distances, Si1···H1 = 3.120 Å and Si2···H2 = 4.060 Å.

172°. The η^2-coordination mode of the Si−Hb bonds is clearly shown by a lengthening of about 24% of these bonds compared to a typical Si−H bond distance of 1.49 Å. However, the Ru−Hb bonds are only slightly longer (by 0.05 Å) than the "classical" Ru−H bonds. The classical hydrides H1 and H2 are turned toward the silicon atoms, with the consequence that the phosphines are cis to each other. This situation is unusual when we note that isomer A is the lowest-energy isomer for RuH$_2$-{(η^2-HSiH$_2$)$_2$X}(PH$_3$)$_2$ with X = C$_6$H$_4$ or (CH)$_2$. The distances between the silicon atoms and the hydrides H1 and H2 are only 2.25 Å, much shorter than the sum of the van der Waals radii of silicon and hydrogen (3.3 Å). This observation suggests that there are weak attractive interactions between the Si and H atoms. On the other hand, the ruthenium−hydride bonds are slightly longer, by 0.011 Å, than those in RuH$_2$(η^2-H$_2$)$_2$(PH$_3$)$_2$.[13h]

Isomer B, which is 32 kJ/mol less stable than A, also has the phosphines in a cis position. The calculated P1−Ru−P2 angle is 97.9°, very similar to the value of 98.4° in isomer A. However,

one phosphine is now trans to a Si−Hb bond, while the other is trans to a hydride, so that isomer B has no symmetry whatsoever (C_1). The two Si−Hb bond lengths are very different; Si1−Hb1 is 0.32 Å longer than a Si−H bond in an isolated silane, similar to the extension found for isomer A, but Si2−Hb2 is longer by a further 0.34 Å, indicating an almost broken bond. The Si2−Hb2 bond is therefore much more activated than Si1−Hb1. This result may also be deduced from the difference between the two Ru−Hb−Si angles, which are 93° for Ru−Hb1−Si1 but 81.6° for Ru−Hb2−Si2 (see Supporting Information). If we suppose that the activation mechanism of an Si−H σ bond on a metallic center begins with the H atom approaching the metal, followed by a rotation of the Si atom toward the metal to form the (η^2-Si−H) complex (see Scheme 1 b), we see that we may use the M−Hb−Si angle as an indicator of the degree of activation of the Si−Hb bond: the smaller the value of this angle, the greater the activation of the Si−H bond. The weak interactions between the silicon atoms and the hydrides H1 and H2 already noted for isomer A do not exist in isomer B. The calculated Si1···H2 and Si2···H1 distances of 3.52 and 3.58 Å, respectively, exceed the sum of the van der Waals radii. Two other silicon−hydrogen distances must be considered for the nonsymmetrical isomer B, but these are also too long to imply a noticeable Si−H interaction (see Table 5).

Isomer C has C_{2v} symmetry; the two Si−Hb and Ru−H bonds lie in a common plane, each hydride being trans to an Si−Hb bond. The other symmetry plane contains the Ru and two P atoms, with the two phosphines occupying the axial sites of the pseudo-octahedron. As expected, the calculated P1−Ru−P2 angle of 169.4° is close to 180°. Two indicators show that the Si−Hb bonds are less activated in isomer C than in the others: the Si−Hb bonds are only 0.23 Å longer than in a free silane, a lengthening of 15% compared to 24% for isomer A, and the value of the Ru−Hb−Si angles (101.6°) is substantially greater than 90°. This reduction of the Si−Hb bond activation, together with the lack of any interaction between the silicon atoms and the hydrides (prevented by the coordination geometry around Ru), leads to isomer C being the least stable of the three; it is 45 kJ/mol above isomer A.

To determine whether the benzene ring plays a role in the relative stability of the three isomers, we reoptimized the geometries of isomers A, B, and C changing the bridging group X to (CH)$_2$. Bond lengths involving ruthenium are changed by less than 0.003 Å for isomer A and by less than 0.015 Å for isomers B and C, while the greatest changes to bond angles are 1° for A, 2.6° for B, and 1.5° for isomer C. No significant change is found for the relative energies of the three isomers. We deduce that there is no particular influence of the benzene ring.
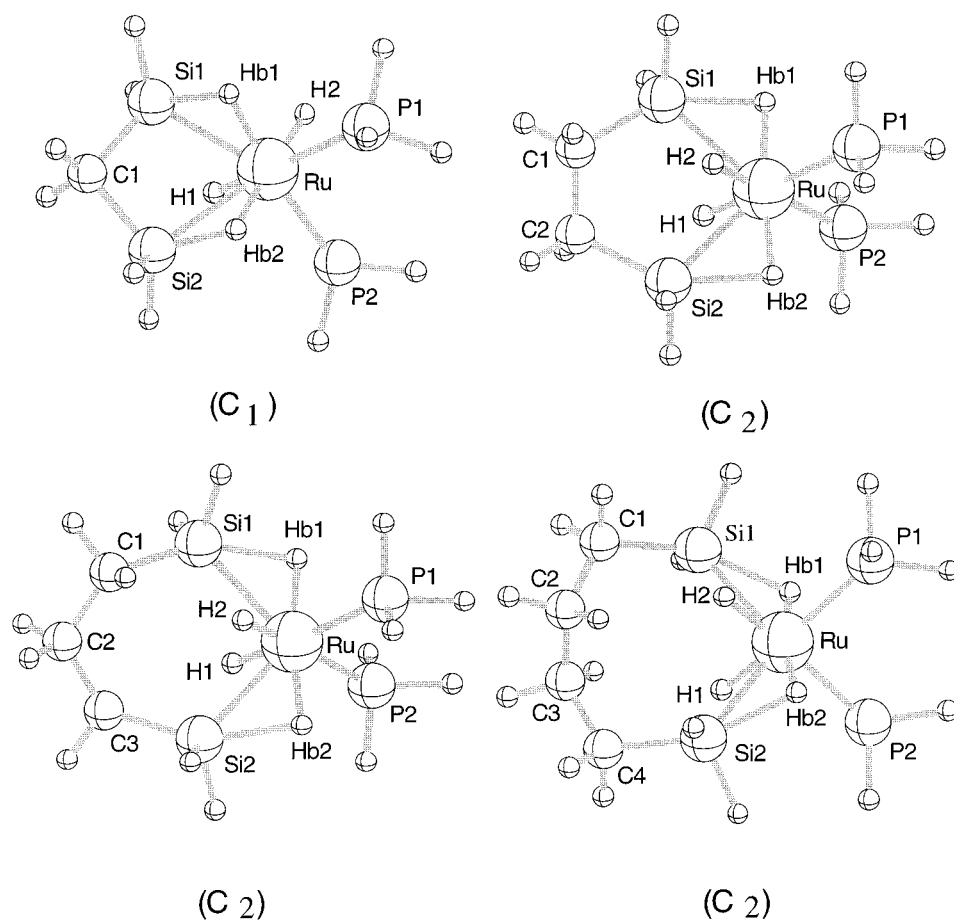
Figure 6. The B3LYP-optimized structures of the $RuH_2\{(\eta^2\text{-}HbSiH_2)_2(CH_2)_n\}(PH_3)_2$ series.

We initially adopted the simplifying assumption that the alkyl groups on both silicon and phosphorus atoms in the real systems could safely be replaced by hydrogen atoms. To verify this assumption, we also optimized the geometries of isomers A and C for the complexes $RuH_2\{(\eta^2\text{-}HSiMe_2)_2C_2H_2\}(PH_3)_2$ and $RuH_2\{(\eta^2\text{-}HSiH_2)_2C_2H_2\}(PMe_3)_2$. There is no influence on the relative energies of the isomers; C remains less stable than A by 42−45 kJ/mol. The only notable difference is the calculated value of the P1−Ru−P2 angle in isomer A. While this angle is around 98−99° for complexes with PH_3 ligands, no matter which bridging group X is present, it increases appreciably to 105.5° when PMe_3 ligands are present, due to the steric bulk of the phosphine; this value is close to the experimental result of 108.8° found with PCy_3 ligands (see section B).

For all of the other bis(silane) complexes studied theoretically, we optimized only the structure corresponding to isomer A. The B3LYP-optimized geometries for the $RuH_2\{(\eta^2\text{-}HSiH_2)_2(CH_2)_n\}$-$(PH_3)_2$ series are displayed in Figure 6, and the corresponding calculated geometrical parameters as well as X-ray data for **4** are listed in Table 4. The geometry optimized for the $n = 2$ species with C_{2v} symmetry proved to be a transition state. Following the imaginary vibrational frequency, one reaches a structure of C_2 symmetry, 13.8 kJ/mol lower in energy, that is a true minimum. In this structure, the C1−C2 bond lies out of the plane formed by the Si1, Si2, and Ru atoms by 9.5°. In the same way, the $n = 3$ and $n = 4$ species belong to the C_2 point group. For these three complexes, the two equivalent Si−Hb bonds are stretched by 0.36−0.39 Å, and the Ru−Hb-Si angles are about 87°, indicating that the degree of activation of the Si−Hb bonds is comparable to that encountered in isomer A of $RuH_2\{(\eta^2\text{-}HSiH_2)_2(C_6H_4)\}(PH_3)_2$. However, we note that the

chelating angle Si−Ru−Si increases steadily from 88.3° to 107.4° with the length of the bridging alkyl chain. As already mentioned, all of these structures are stabilized by weak attractive interactions between the Si and the classical hydrides H1 and H2, as shown by the short Si···H distances in the range 2.15−2.58 Å. The complex with a single bridging CH_2 group is a special case in the series because its B3LYP-optimized geometry has no symmetry. If C_2 symmetry is imposed, with two equivalent Si−Hb bonds, the four-membered metallocycle would be too strained. A C_1 structure that is 16.3 kJ/mol lower in energy is found when unconstrained optimizations are performed.

To study the influence of the chelating chain X, we also optimized the geometries of bis(silane) complexes in which the alkyl chain was replaced by disiloxane ligands. The B3LYP-optimized structures of $RuH_2\{(\eta^2\text{-}HSiH_2)_2O\}(PH_3)_2$ and RuH_2-$\{(\eta^2\text{-}HSiH_2)_2O(SiH_2)O\}(PH_3)_2$ are presented in Figure 7, and the corresponding geometrical parameters, together with the X-ray crystal structure results for **6**, are listed in Table 6. For the case where X = O, a C_{2v} stationary point was located that was shown to be a transition state with a single imaginary vibrational frequency ($243i$ cm⁻¹); the only true minimum that could be located has no symmetry (C_1) and is 15.5 kJ/mol lower in energy. One of the Si−Hb bonds, Si1−Hb1, is suitably activated because its length is 0.29 Å greater than a classical Si−H bond in a free silane and the Ru−Hb1−Si1 angle is 90.3°, whereas the other, Si2−Hb2, is not particularly activated because it is stretched by only 0.11 Å and the corresponding Ru−Hb2−Si2 angle is 105°. This situation is the result of an excessive strain imposed in the four-membered metallocycle with a chelating Si−Ru−Si angle of only 65.2°. As a conse-
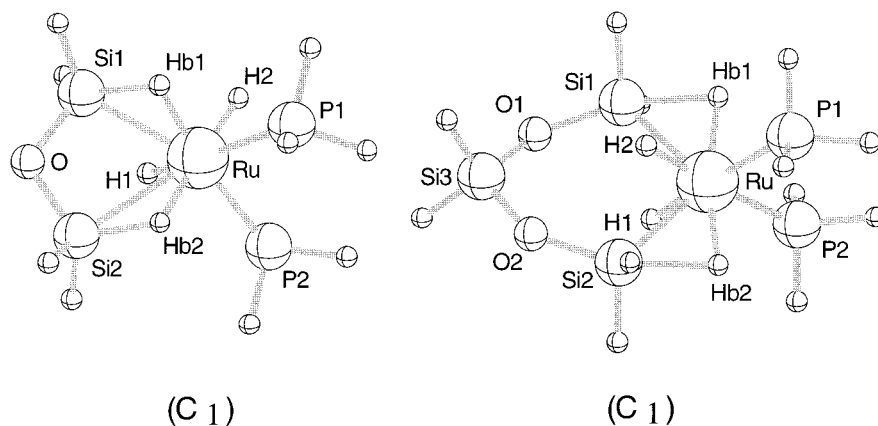
Figure 7. The B3LYP-optimized structures of $RuH_2\{(\eta^2\text{-}HbSiH_2)_2X\}(PH_3)_2$ with X = O, $OSiH_2O$.

Table 6. Calculated Geometrical Parameters[a] for the $RuH_2((\eta^2\text{-}HSiH_2)_2X)(PH_3)_2$ Siloxane Series and X-ray Data for $RuH_2((\eta^2\text{-}HSiMe_2)_2OSiMe_2O)(PCy_3)_2$ **6**

	X = O, B3LYP	X = $OSiH_2O$, B3LYP	X = $OSiMe_2O$, X-ray for **6** (180 K)
Ru−Hb1	1.658	1.670	1.62(4)
Ru−Hb2	1.805	1.667	1.58(4)
Si1−Hb1	1.784	1.826	1.77(4)
Si2−Hb2	1.596	1.839	1.81(3)
Si1···H1	2.125	2.170	2.25(3)
Si2···H2	4.181	2.168	2.04(3)
Si1···H2	2.913	2.484	2.43(3)
Si2···H1	2.670	2.426	2.32(3)
Ru−Si1	2.442	2.451	2.4841(7)
Ru−Si2	2.700	2.447	2.4336(7)
Ru−H1	1.627	1.632	1.55(4)
Ru−H2	1.614	1.634	1.51(3)
Ru−P1	2.377	2.382	2.4540(7)
Ru−P2	2.340	2.382	2.4614(6)
Ru−Hb1−Si1	90.3	89.0	94.0(18)
Ru−Hb2−Si2	105.0	88.4	91.7(17)
Hb1−Ru−Hb2	92.4	167.0	169.2(17)
Hb1−Ru−H1	105.0	100.4	90.7(18)
Hb1−Ru−H2	86.5	88.5	100.3(18)
Hb2−Ru−H1	102.8	88.4	94.1(18)
Hb2−Ru−H2	174.3	99.5	88.6(17)
Si1−Ru−Si2	65.2	100.5	97.25(2)
H1−Ru−H2	82.9	99.6	97.8(18)
P1−Ru−P2	96.1	100.1	108.36(2)
P1−Ru−Si1	126.0	124.3	115.29(2)
P1−Ru−Si2	121.6	105.9	108.76(2)
P2−Ru−Si1	136.9	104.5	108.09(2)
P2−Ru−Si2	103.1	123.6	119.09(2)
P1−Ru−H1	166.9	174.7	174.7(12)
P1−Ru−H2	85.0	80.3	77.0(14)
P2−Ru−H1	77.9	80.4	76.9(12)
P2−Ru−H2	84.9	175.4	174.4(13)

[a] See Figure 7 for labeling of the atoms. Distances are in Å and angles in degrees.

quence, the classical hydride H2 is located far from the silicon atoms and the attractive Si···H interactions are possible only with H1. The complex in which X = $OSiH_2O$ behaves differently. Although it also belongs to the C_1 point group, the two Si−Hb bonds are activated to approximately the same extent. The degree of activation of the two Si−Hb bonds is comparable to that observed in isomer A of $RuH_2\{(\eta^2\text{-}HSiH_2)_2(C_6H_4)\}(PH_3)_2$.

Vibrational wavenumbers and infrared intensities calculated at the B3LYP level of theory are presented in Table 7 for the Ru−Hb and Ru−H stretching modes of the bis(silane) model complexes studied in this work. The most intense band in all cases is the Ru−Hb antisymmetric stretch.

Calculated values of the binding energies for eight different compounds containing the $(HSiH_2)X$ ligand to the unsaturated $RuH_2(PH_3)_2$ fragment are reported in Table 8. Since the products are more stable than the reactants, the energy differences are negative. Several different energetic quantities are displayed. ΔE represents the difference in electronic energy, each fragment being in its ground-state geometry optimized at the same level of theory. The zero-point energy (ZPE) and thermal enthalpy ($T = 298.15$ K and $P = 1$ atm) correction terms may be computed from the results of the vibrational frequency calculations. The reaction enthalpy $\Delta H°$ can then be derived. While absolute errors of the order of 20 kJ/mol may be present, we expect that trends in the values for a related series should be rather reliable. We therefore conclude that there are well-established differences in the electronic binding energies as a function of the bridging group X, as these vary from 130 to 192 kJ/mol.

D. Reactivity Studies. With H_2, CO, or ^tBuNC (see Scheme 5). 1 was shown previously to generate the dicarbonyl complex $RuH_2(CO)_2(PCy_3)_2$ (**7**) by H_2/CO exchange.[13c] Similar behavior is observed in the case of **2a,b**, **5**, and **6** as they readily react with CO to produce the same ruthenium complex **7** with elimination of the corresponding disilane. However, a very slow reaction is observed in the case of **4** (less than 10% of **7** is obtained after bubbling CO for 2 min), whereas no reaction occurs in the case of **3** after prolonged CO bubbling. Under 3 bar of CO, **3** decomposes to a mixture of compounds from which $Ru(CO)_3(PCy_3)_2$ was characterized as the major product.

Elimination of the bis(silane) ligands can also be achieved by addition of 2 equiv of ^tBuNC to a C_6D_6 or pentane solution of **2** or **4**−**6**, and the dihydride complex $RuH_2(^tBuNC)_2(PCy_3)_2$ (**8**) is formed quantitatively. **8** can also be isolated from **1** in 92% yield and is characterized in particular by a hydride resonance at δ −9.49 (t, $J_{P-H} = 24$ Hz). Stronger coordination of the bis(silane) ligand in **3** is again demonstrated since partial conversion into **8** is observed. In an attempt to substitute only one $(\eta^2\text{-}Si-H)$ we added 1 equiv of ^tBuNC to a solution of **2a**, **4**−**6**: a mixture of the starting complex and **8** was obtained. However, for **2b**, a mixture of **8** and a new complex tentatively formulated as $RuH_2[(\eta^2\text{-}HSiPh_2)OSi(Ph_2)H](^tBuNC)(PCy_3)_2$ was obtained. In all of these reactions, the elimination of the disilanes was confirmed by ^1H NMR and GC.

The bis(silane) complexes are obtained in good yield from the reaction of **1** with the corresponding disilane. The reaction is totally reversed in the case of **2a** and **2b** after bubbling H_2 for 2 or 10 min respectively: **1** and the disiloxane are obtained quantitatively as shown by NMR spectroscopy. The same reaction is observed for **5** and **6**, but after 2 min, only 50% of

Table 7. Vibrational Frequencies^a (cm^{-1}) and Infrared Intensities^b (km/mol) for the Ru−H and Ru−Hb Stretching Modes in RuH$_2$((η^2-HbSiR$_2$)$_2$X)(PR$_3$)$_2$

	X = C$_6$H$_4$		X = (CH$_2$)$_2$		X = (CH$_2$)$_3$		X = O			X = OSiH$_2$O	X = OSiMe$_2$O
	R = R′ = H B3LYP	R = Me R′ = Cy exptl	R = R′ = H B3LYP	R = Me R′ = Cy exptl	R = R′ = H B3LYP	R = Me R′ = Cy exptl	R = R′ = H B3LYP	R = Me R′ = Cy exptl	R = Ph R′ = Cy exptl	R = R′ = H B3LYP	R = Me R′ = Cy exptl
Ru−H as stretch	2013 (80)	1969	2016 (97)	1981	2065 (84)	1994	2018 (108)	1969	1976	2007 (103)	1955
Ru−H s stretch	2018 (108)	1985	2022 (89)	2012	2063 (57)	1961	2040 (76)	2045	2019	2020 (100)	2045
Ru−Hb as stretch	1769 (208)	1778	1761 (236)	1773	1799 (214)	1803	1632 (238)	1699	1670	1839 (245)	1798
Ru−Hb s stretch	1968 (10)	–	1962 (12)	–	1990 (6)	–	1955 (100)	–	–	2015 (8)	–

^{a} As stands for asymmetric and s for symmetric. ^{b} Intensities are in parentheses.

Table 8. Calculated Binding Energies (kJ/mol) of (HSiH$_2$)$_2$ X in the RuH$_2$((η^2-HSiH$_2$)$_2$X)(PH$_3$)$_2$ Complex at the DFT/B3LYP Level of Theory

X	(CH)$_2$	C$_6$H$_4$	CH$_2$	(CH$_2$)$_2$	(CH$_2$)$_3$	(CH$_2$)$_4$	O	O(SiH$_2$)O
ΔE	−192	−186	−130	−169	−140	−133	−140	−189
ΔE + ZPE	−183	−178	−120	−159	−130	−123	−129	−178
$\Delta H°$		−181	−125	−164	−134	−127		−183

Scheme 5. Reactivity of **2−6** with H$_2$, CO, ^{t}BuNC

Scheme 6. Reactivity of **2−6** with PPh$_3$ and Ppyl$_3$
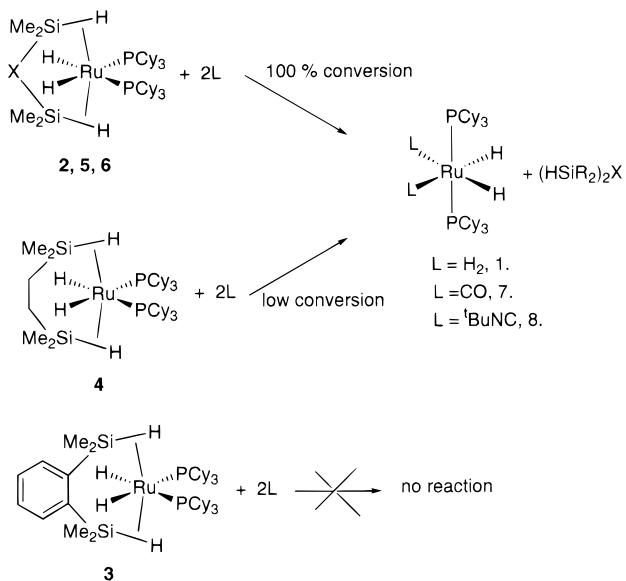
1 is produced. A reaction time of 50 min and pressure of 3 bar are required to reach 10% conversion of **4**, whereas after 24 h, **3** remains unchanged.

With Various PR$_3$ (see Scheme 6). We have compared the effect of the addition of various phosphines to complexes **2−6**. We have used phosphines with various steric and electronic properties: bulky and basic phosphines such as P^{i}Pr$_3$ or phosphines displaying a smaller cone angle such as PPh$_3$ or Ppyl$_3$, the latter one being a strong π-acceptor.[33] The study of the reactivity of **2−6** toward small molecules such as H$_2$ or CO demonstrated that **3** and, to a lesser extent, **4** had the greatest stability.

When **3** or **4** are treated with 1 equiv of PR$_3$, the bis(silane) ligand remains bound to the ruthenium via two σ- Si−H bonds and substitution of one PCy$_3$ is achieved. The new complexes [RuH$_2$\{(η^2-HSiMe$_2$)$_2$(C$_6$H$_4$)\}(PCy$_3$)(PR$_3$)] (with R = Ph (**3Ph**), and R =pyl (**3pyl**) and [RuH$_2$\{(η^2-HSiMe$_2$)$_2$(CH$_2$)$_2$\}(PCy$_3$)-(PR$_3$)] (with R = Ph (**4Ph**), and R =pyl (**4pyl**) have been isolated in good yields (80−85%) and fully characterized. In

(33) (a) Moloy, K. G.; Petersen, J. L. *J. Am. Chem. Soc.* **1995**, *117*, 7696. (b)Rodriguez, V.; Donnadieu, B.; Sabo-Etienne, S.; Chaudret, B. *Organometallics* **1998**, *17*, 3809.

the case of **4Ph**, an X-ray determination was obtained (see Tables 2 and 3). The spectroscopic data are reported in Tables 9 and 10. All of the complexes present similar ^{31}P NMR spectra: an AB or AX pattern with a small J_{PP} value (23 to 30 Hz) in agreement with a cis arrangement of the two different phosphines. The ^{1}H NMR spectra in the hydride region show a pseudotriplet near δ −7.5 for the two η^2-bound Si−H protons and a doublet of doublets for each hydride or a pseudotriplet in

Table 9. Selected ^{1}H NMR Data for the Mixed Phosphine Complexes [RuH$_2${(η^2-HSiMe$_2$)$_2$X}(PCy$_3$) (PR$_3$)], **3R−6R**

			Si−*Me*		Si−*H*[b]		Ru−*H*[c]				
X	R	complexes[a]	δ_{Me}		δ_{SiH}	J_{HP} (Hz)	δ_{RuH}	J_{HP} (Hz)		δ_{RuH}	J_{HP} (Hz)
C$_6$H$_4$	Ph	**3Ph**	0.79	1.22	−7.21	14	−10.47	44.1	28.2	−10.91	21.9	52.7
C$_6$H$_4$	pyl	**3pyl**	0.78	1.09	−7.30	10	−9.79	17.0	93.6	−10.27	38.3	29.8
(CH$_2$)$_2$	Ph	**4Ph**	0.54	0.97	−7.68	14	−11.10	45.2	30.5	−11.47	24.2	53.6
(CH$_2$)$_2$	pyl	**4pyl**	0.52	0.82	−7.87	15	−10.27	20.0	93.4	−11.01	38.2	30.4
(CH$_2$)$_3$	Ph	**5Ph**	0.36	0.78	−8.07	13	−10.70	42.3	23.1	−11.31	18.2	55.6
OSi(Me$_2$)O	Ph	**6Ph**	0.56	0.99	−8.70	14	−9.68	43.8	24.6	−10.31	18.2	54.6

[a] C$_6$D$_6$, 288 K, 400 MHz. [b] Pseudotriplet. [c] Doublet of doublet.

Table 10. Selected ^{31}P and ^{29}Si NMR and IR Data for the Mixed Complexes [RuH$_2${(η^2-HSiMe$_2$)$_2$X}(PCy$_3$) (PR$_3$)], **3R−6R**

			^{31}P NMR[a,b]			^{29}Si NMR[a,c]			IR[d]	
X	R	complexes	δ_{PCy_3}	δ_{PR_3}	J_{PP}	δ_{Si}	J_{SiH}	J_{SiP}	ν_{RuH}	ν_{RuHSi}
C$_6$H$_4$	Ph	**3Ph**	53.3	54.8	23	6.59	64	8.2	1973	1948	1787
C$_6$H$_4$	pyl	**3pyl**	53.7	128.7	28	5.65	66	7.8	1974	1953	1805
(CH$_2$)$_2$	Ph	**4Ph**	53.7	55.2	28	14.7	64	7.7	2008	1989	1768
(CH$_2$)$_2$	pyl	**4pyl**	53.6	128.5	30	14.0	63	7.2	1990 (br)		1770
(CH$_2$)$_3$	Ph	**5Ph**	52.8	54.0	20					
OSi(Me$_2$)O	Ph	**6Ph**	50.8	52.7	20					

[a] C$_6$D$_6$. 288 K. [b] 161.99 MHz. [c] 79.5 MHz. [d] Nujol (cm^{-1}).

Table 11. Selected NMR Data for [RuH$_2${(η^2-HSiMe$_2$)$_2$X}(PR$_3$)$_2$], **3R$_2$, 4R$_2$**

			^{1}H NMR[a,b]			^{31}P NMR[a,c]	^{29}Si NMR[a,d]		
X	R	complexes	δ_{SiMe}	δ_{SiH}	δ_{RuH}	δ_P	δ_{Si}	J_{SiP} (Hz)	J_{SiH} (Hz)
C$_6$H$_4$	Ph	**3Ph$_2$**	0.93	−7.10	−10.46	51.9	8.12	8.2	63
C$_6$H$_4$	pyl	**3pyl$_2$**	0.96	−6.47	−8.83	131.3	8.80[f]	7.6	61
(CH$_2$)$_2$	Ph	**4Ph$_2$**	0.07[e]	−7.60	−10.92	54.8	16.4	7.7	64
(CH$_2$)$_2$	pyl	**4pyl$_2$**	0.42	−7.8[g]	−9.4[g]	125.9			

[a] C$_6$D$_6$, 288 K. [b] 400 MHz. [c] 161.99 MHz. [d] 79.5 MHz. [e] CD$_2$Cl$_2$. [f] 253 K. [g] Broad.

the case of **3pyl** and **4pyl**. The three signals integrate in a 2:1:1 ratio. As an example, in the case of **3pyl**, the three signals simplify to three doublets upon selective decoupling of each phosphine. The pseudotriplet at δ −7.30 is assigned to the two η^2-bound Si−H protons with $J_{H-P(PCy_3)}$ = 9 Hz and $J_{H-P(Ppyl_3)}$ = 11 Hz. The signal at δ −9.79 is attributed to the hydride trans to Ppyl$_3$ (the large J_{H-P} value is in agreement with the strong π-acceptor properties of the Ppyl$_3$), and the signal at δ −10.27 to the hydride trans to PCy$_3$. The methyls bound to the silicons are now inequivalent, due to the presence of the two different phosphines. The ^{29}Si NMR and IR data are very similar to the analogues **3** and **4** as can be seen from Table 10. The X-ray structure of **4Ph** was determined at 180 K (see Tables 2 and 3). It is very similar to the analogous compound **4** with the two PCy$_3$. The substitution by PPh$_3$ induces a reduction of only 3° for the P−Ru−P angle, despite a much smaller Tolman angle for PPh$_3$ (145° compared to 170° for PCy$_3$). To confirm the weak steric effect induced by the phosphines, we have synthesized the analogous complex [RuH$_2${(η^2-HSiMe$_2$)$_2$(CH$_2$)$_2$}-(PPh$_3$)$_2$] (**4Ph2**) with 2 PPh$_3$ ligands. It can be obtained in high yield by using the same strategy as for the synthesis of **1**, i.e., addition of 1 equiv of the disilane to Ru(COD)(COT) in the presence of 2 equiv of the desired phosphine under H$_2$ atmosphere. We could thus isolate in good yields the complexes [RuH$_2${(η^2-HSiMe$_2$)$_2$X}(PR$_3$)$_2$] (X = C$_6$H$_4$, R = Ph (**3Ph2**) and R = pyl (**3pyl2**); X = (CH$_2$)$_2$ R = Ph, **4Ph2**; R = pyl, **4pyl2**) (see Table 11 for spectroscopic data). **4Ph2** was characterized by an X-ray determination at 150 K (see Tables 2 and 3) which corroborates the absence of any influence of the nature of the phosphine ligands on the structure of the compounds. The variation of the basicity of the phosphines is better illustrated by the highfield shift of the classical hydride signals in the ^{1}H

NMR spectra (PCy$_3$ > PPh$_3$ > Ppyl$_3$). However, the J_{Si-H} values are too close to allow any comment.

Treatment of **2a,b** with 1 equiv of PCy$_3$ gave the dihydride-(dihydrogen) complex RuH$_2$(H$_2$)(PCy$_3$)$_3$ after 3 days, and elimination of the corresponding disiloxane. RuH$_2$(H$_2$)(PCy$_3$)$_3$ was characterized by ^{1}H and ^{31}P NMR spectra. It has previously been synthesized by addition of 3 equiv of PCy$_3$ to Ru(COD)-(COT) under H$_2$ pressure.[34] A similar reaction also occurred in the case of Ppyl$_3$. Addition of 1 equiv of Ppyl$_3$ to a C$_6$D$_6$ solution of **2a,b** was shown by ^{1}H and ^{31}P NMR to give rise to a mixture of compounds, including the corresponding disiloxanes and a new compound stabilized by three phosphines RuH$_2$(H$_2$)(Ppyl$_3$)-(PCy$_3$)$_2$ (**9**). This complex could be directly synthesized and isolated by addition of 1 equiv of Ppyl$_3$ to **1**. It is in particular characterized by ^{31}P NMR: a triplet at δ 119.9 is observed for the resonance of the Ppyl$_3$ and a doublet at δ 62.7 for the resonance of the PCy$_3$ with a J_{P-P} coupling constant of 13 Hz indicative of two equivalent PCy$_3$ ligands cis to the Ppyl$_3$. When 2 or more equiv of Ppyl$_3$ are added to a C$_6$D$_6$ solution of **2a,b**, elimination of the disiloxane was again observed, and the new dihydride RuH$_2$(Ppyl$_3$)$_4$ (**10**) was detected. This complex could be isolated as a white solid by addition of 4 equiv of Ppyl$_3$ to Ru(COD)(COT) under dihydrogen pressure. It was fully characterized by NMR (a multiplet at δ −8.6 for the two hydrides and two broad signals at δ 119.1 and 117.6 for the four Ppyl$_3$). This complex was also obtained by addition of an excess of Ppyl$_3$ to **3** or **4**.

Addition of PPh$_3$ or Ppyl$_3$ to **5** or **6** resulted in behavior intermediate between that of **2** and those of **3−4**. Thus addition of 1 equiv of PPh$_3$ to **5−6** leads to the formation of the mixed compounds [RuH$_2${(η^2-HSiMe$_2$)$_2$X}(PCy$_3$)(PPh$_3$)] **5Ph** and **6Ph**

(34) Chaudret, B.; Poilblanc, R. *Organometallics* **1985**, *4*, 1722.

respectively, as observed in the case of **3**−**4**. However, addition of 1 equiv of Ppyl₃ gives a mixture of compounds among which [RuH₂{(η²-HSiMe₂)₂X}(PCy₃)(Ppyl₃)] (**5pyl**) or **6pyl** were characterized by analogy of their NMR data to **3pyl** and **4pyl** together with RuH₂(H₂)(Ppyl₃)(PCy₃)₂ (**9**) already described during the reaction of **2a** with Ppyl₃. The NMR data of **5Ph**, **6Ph**, **5pyl**, and **6pyl** are reported in Tables 9 and 10.

Discussion

In this paper we describe several examples of a new family of complexes stabilized by the coordination of a disilane ligand via two σ Si−H bonds. Both the bridge between the two silicons and the phosphine ligands were modified, to evaluate their influences on the structural properties and on the stability and reactivity. The first aspect of these molecules that needs comment is the coordination geometry at the Ru center. In both the X-ray Determinations and Theoretical Calculations above (B and C, respectively), we have described a pseudo-octahedral arrangement about Ru, where the η²-Si−H bond is considered as a single ligand, and the two phosphines adopt an unusual cis arrangement. The essential structural features revealed by X-ray diffraction are identical to those found by calculation (see Table 4), both qualitatively and quantitatively, with differences between experimental and theoretical values of only a few hundredths of an Å for bonded distances or tenths of a degreee for angles; we exclude the P−Ru−P angle here, as the PH₃ ligands are less sterically demanding than PCy₃, and note that the location of H atoms by X-ray diffraction is subject to relatively large uncertainties.

In RuH₂(H₂)₂(PCy₃)₂ (**1**), the two phosphines are trans, a feature which has been interpreted as a consequence of their steric bulk. Unfortunately the X-ray data we have obtained to date for **1**, while showing a trans position for the phosphines, do not enable us to locate the hydrogen atoms, even at low temperature. During the course of our studies on the reactivity of **1**, some of us have already reported X-ray data concerning ruthenium complexes accommodating two trans PCy₃ ligands.[13b,e,15] The highest distortion from a trans configuration is observed for the complex [RuH₂{(η⁴-HSiMe₂(CH=CHMe)}-(PCy₃)₂] published very recently.[15] In this case, the P−Ru−P angle is reduced to 145.30(6)°, and the J_{P-P} coupling constant of 206 Hz, measured by ³¹P NMR, is still in agreement with a trans configuration. To evaluate the steric influence of the phosphine substituents, we have chosen to prepare compounds in which one or two PCy₃ could be substituted by one or two triphenylphosphines. These two phosphines present very different cone angles, i.e., 170° for PCy₃ and 145° for PPh₃. It was possible to isolate and characterize by X-ray analysis, the series [RuH₂{(η²-HSiMe₂)₂(CH₂)₂}(PR₃)(PR′₃)] R=R′=Cy, **4**, R=Cy, R′=Ph, **4Ph**, R=R′=Ph, **4Ph2**. They all present similar structures, and it is striking that the P−Ru−P angle varies so little with the nature of the phosphine, with the X-ray values lying in a narrow range between 104° (compound **4Ph2**) and 108° (compound **4**). The computed angles are within this range if the phosphine contains alkyl substituents even as small as methyl. We deduce that steric factors have little direct influence on the P−Ru−P angle and that the origin of the unusual coordination geometry must be found elsewhere. By using the tripyrrolylphosphine Ppyl₃, a phosphine which has the same cone angle as PPh₃ but which is a strong π-acceptor,[33] similar compounds (**3pyl**, **3pyl2**, **4pyl**, **4pyl2**) were obtained as deduced by their spectroscopic properties. The main differences are demonstrated by NMR data. An increase of the electron density on the metal induces a highfield shift for the hydride signals in

the ¹H NMR spectra and of the Si signals in the ²⁹Si NMR spectra. This effect is stronger for the classical hydrides trans to the more basic phosphine (PCy₃ > PPh₃ > Ppyl₃). However, little effect is observed on the J_{Si-H} values, which measure the activation of the Si−H bond.

The most stable isomer of **3**, which according to the theoretical studies is isomer A, lies about 45 kJ/mol lower in energy than isomer C which contains trans phosphines. Attention has already been drawn to the relatively close approach of the "classical" hydrides H1 and H2 to the silicon atoms; the calculated distances of around 2.25 Å (Table 4) are substantially less than the sum of the van der Waals radii. There does not appear to be any geometrical constraint which has imposed these close contacts, as they are rather constant in the series containing one, two, three, or four CH₂ units linking the two Si atoms (Table 4), despite the substantial differences in size of the four bidentate ligands. The natural interpretation is that these close H···Si contacts are a stabilizing feature of the overall structure. Support for this interpretation is provided by the Mulliken population analysis, which shows small but certainly nonnegligible positive overlap populations between H1 and Si1 of 0.027 in **3**. To place this figure in context, the Si1−Hb1 overlap population in **3** is 0.15, while in the free ligand it is 0.39. Similar interactions are present in the MCp₂XH(SiR₃) complexes studied very recently by Fan and Lin (M is Nb or Ta, and X is SiR₃, Cl, H, or CH₃);[35] these authors report hydride−Si nonbonded distances of around 2.2 Å. It is clear from the data in Table 5 that this stabilizing interaction is absent in isomers B and C, since the closest H···Si distances in those cases are greater than 3 Å. The X-ray data obtained for the five compounds **3**, **4**, **4Ph**, **4Ph2**, and **6** show nonbonding Si···H distances from 2.04 to 2.43 Å for the extreme values, with at least two Si···H distances around 2.15 Å for each compound. Theoretical calculations at the Hartree−Fock level on ReH₆(SiR₃)(PPh₃) and ReH₂(CO)-(SiPh₃)(PMe₂Ph)₃ have previously shown that interactions between Si and H are still present, even if they are separated by 2.1 to 2.3 Å.[36]

These short nonbonding Si···H distances are presumably of vital importance in the exchange process observed by NMR which involves the hydrides and the (η²-Si−H) hydrogens. A rather easy exchange process needs to operate since (i) we have shown that addition of the deuterated disilane DSiMe₂(CH₂)₃-SiMe₂D to **1** results in 50% deuterium incorporation in each hydride resonances of **5-d** and (ii) the ¹H NMR spectra of **2**−**6** are temperature dependent. Examination of the literature shows that fast exchange at room temperature is observed in compounds bearing these two types of hydrides (M−H and M-(η²-Si−H)) and the exchange is characterized by barriers in the range 35−50 kJ/mol.[24−26,37] The two dinuclear complexes Cp*₂-Ru₂(SiPh₂CH=CH₂)(μ-η²-HSiPh₂)(μ-H)(H) and Cp*₂Ru₂(μ-η²-HSiⁱBu₂)(μ-η²-HSiHPh)(μ-H)(H) were previously reported as nonfluxional at room temperature.[24a,38] In our case, fast exchange at room temperature is only observed for **2a,b** with $\Delta G^{\ddagger}$ close to the higher limit, i.e., 47.5 and 51 kJ/mol, respectively. This fluxionality is markedly reduced in the case of **3**−**6**, as two different signals are observed at room temperature for the hydrides and the (η²-Si−H) hydrogens: fast exchange is now observed at much higher temperature (376 K > Tc > 333 K) with much higher $\Delta G^{\ddagger}$ values (between 62.5 and 68.4 kJ/mol). The main route commonly invoked in the literature to explain

(35) Fan, M. F.; Lin, Z. *Organometallics* **1998**, *17*, 1092.

(36) Lin, Z.; Hall, M. B. *Inorg. Chem.* **1991**, *30*, 2569.

(37) Fryzuk, M. D.; Rosenberg, L.; Rettig, S. J. *Organometallics* **1996**, *13*, 2871.

(38) Takao, T.; Suzuki, H.; Tanaka, M. *Organometallics* **1994**, *13*, 2554.

the exchange between M–H and M–(η^2-Si–H) goes through the breaking of a Si–H bond, resulting in oxidative addition and then intramolecular rearrangement via for example dihydrogen species.[10b,23b,26,37] It is noteworthy that in our systems the fragment RuH$_2$(PCy$_3$)$_2$ can stabilize either (η^2-Si–H) or (η^2-H–H) species, but we were not able to detect any dihydrogen intermediates. More studies are needed to understand in detail the mechanism of the exchange process operating in our systems, and new NMR experiments and theoretical calculations are planned. This should enable us in particular to discriminate between phosphine or Si–H decoordination; however, in any event the short nonbonding Si···H distances play an important role and five-coordinate silicon species could be involved at least as transition states.

Vibrational spectroscopy is a powerful tool for the characterization of silane complexes containing (η^2-Si–H) bonds, as these species display intense bands in the range 1650–1800 cm^{-1} that are shifted to substantially lower frequencies than in the free ligands. The calculated vibrational frequencies are in quite satisfactory agreement with the experimental values (Table 7), being within some 50 cm^{-1}, or 2.5%, in all cases. In previous work, some authors have assigned these vibrations as essentially Si–Hb stretching modes and used the change in frequency from the isolated ligand value as an indication of the extent of activation (extension) of the (η^2-Si–H) bonds.[5g,22,24a] However, analysis of the vibrational motions predicted by the B3LYP calculations implies that the motion is better described as a Ru–Hb stretching. There is extensive mixing of several different vibrational motions, and no mode corresponds closely to a stretch of the Si–Hb bond. We note that localized orbital plots show the presence of an almost classical Si–Hb–Ru three-center two-electron bond. Moreover, the Ru–Hb1 distance, calculated to be 1.681 Å in **3**, is only 3% greater than the classical Ru–H bond length, whereas the Si–Hb distance of 1.848 Å is some 24% greater than the noncomplexed Si–H bond lengths. These geometrical considerations imply that the "bridging" Hb atom is more strongly linked to Ru than to Si, and thus it is reasonable for the highest-frequency mode of this unit to involve primarily a Ru–Hb stretching motion. It is satisfying to note that the Ru–Hb stretching frequencies for the series containing an aliphatic backbone linking the two silicon atoms increase steadily with the length of that backbone (Table 7), while the Ru–Hb distances in these compounds decrease steadily (Table 4).

We have presented here simple reactivity studies on **2–6**, and the results can be correlated with the structural properties of the compounds. **2a,b** are by far the least stable compounds, and the corresponding disiloxane is readily eliminated by reaction with small molecules such as H$_2$ or CO or with phosphines. In contrast, the disilane ligand is less reactive in **3** probably as the result of the steric hindrance resulting from the ring between the two silicons: this is specially highlighted by the absence of reactivity of **3** with CO. The chelate effect, already pointed out by Schubert,[39] is maximized when two groups bridge the two silicons as in **3** and **4**, resulting formally in five-membered ring compounds. Thus, **4** exhibits a behavior similar to that of **3**, whereas **5** and **6** are intermediate between **2** and **3–4**. It should be noted that **2a,b** are nonsymmetrical complexes from theoretical calculations but **3–6** are symmetrical from spectroscopic, X-ray, and theoretical data. Surprisingly, **2a,b** which show the lowest $J_{\text{Si–H}}$ values are the most reactive and display the lowest barrier to activation for the hydride exchange process. This may result from the additional weak

nonbonding Si···H interactions which are present in **3–6**, highlighting the role of such interactions in the reactivity of σ complexes.

This trend of reactivity is supported by calculated binding energies for the bidentate silane ligand to the RuH$_2$(PH$_3$)$_2$ fragment (Table 8). We note that the binding energy (ΔE) calculated for two η^2-H$_2$ ligands with the same theoretical procedure is 149 kJ/mol, showing that the Si–H bond in the most stable complexes is bound more strongly than molecular hydrogen, consistent with the method of preparation of the bis(silane) complexes by displacement of molecular H$_2$ from RuH$_2$-(H$_2$)$_2$(PR$_3$)$_2$ (section A).

For the four compounds studied here that contain an aliphatic backbone, there is a striking variation in binding energy with the length of the (CH$_2$)$_n$ chain, the compound with $n = 2$ being notably more (thermodynamically) stable than the others. Binding energies for compounds containing an unsaturated (CH)$_2$ backbone are higher than for the aliphatic systems. We believe these differences to be consequences of the geometrical reorganization (or relaxation) imposed upon the bis(silane) ligand by complexation. To test this hypothesis, we calculated the energy differences between a free ligand in its optimized geometry and one in which the skeletal geometrical parameters are fixed at the values found in the complex. The following results were obtained (kJ/mol); 2 for X is C$_6$H$_4$, 8 for (CH$_2$), 9 for OSiH$_2$O, 11 for (CH$_2$)$_2$, 19 for (CH)$_2$, 27 for O, 34 for (CH$_2$)$_4$, and 35 for (CH$_2$)$_3$. The corrected or intrinsic binding energies implied for the complexes with X = (CH$_2$)$_n$, $n = 2$, 3, or 4, are thus rather constant, at 180, 175, or 167 kJ/mol, respectively (we have neglected here any differences in the geometry of the ruthenium-containing fragment). The high thermodynamic stability of **4** ($n = 2$) arises because the (CH$_2$)$_2$ bridging group produces a ligand that in a geometrical sense is relatively well-prepared for binding to Ru; while H$_3$Si(CH$_2$)$_2$-SiH$_3$ has a planar (C_{2h}) skeleton as a free molecule, the Si–C–C–Si dihedral angle in complex **4** is 45°, not far from a gauche conformation, so that the energy penalty for ligand preparation is small. However, that penalty is larger for **5** (X = (CH$_2$)$_3$), for which the Si–C–C–C dihedral angle of 36° is appreciably further from a gauche conformation.

The relatively low thermodynamic stabilities and C_1 symmetries for the two complexes containing a single atom as the bridging group, X = CH$_2$ or O, may also be understood from similar considerations. Such small bridges do not allow the SiH groups to attain optimal positions for formation of two (η^2-Si–H) bonds, and the best energetic compromise is found by lowering the symmetry, and the result is that one SiH group is only weakly coordinated as an (η^2-Si–H) bond (note the Ru–Hb distances of 1.663 and 1.807 Å for X = CH$_2$ (Table 4), or 1.658 and 1.805 Å for X = O (Table 6), compared to the two equal Ru–Hb distances of 1.683 Å where X is (CH$_2$)$_2$.

Conclusion

The major advance reported in this article is the isolation of mononuclear bis(silane) complexes stabilized by two σ Si–H bonds thanks to the utilization of potentially chelating disilanes. It is noteworthy that full oxidative addition of the disilane was never observed in any of the reactions we have described here. Enhanced stabilization derives from nonbonding H–Si···H interactions, as shown by X-ray diffraction and theoretical calculations. The chelate effect contributes to the observed stability of the compounds, independent of the nature of the phosphine ligands. The Ru–(η^2-H–Si) bond can be described by several criteria among which the values of $J_{\text{Si–Hb}}$, $\nu_{\text{Ru–Hb}}$,

(39) Schubert, U.; Gilges, H. *Organometallics* **1996**, *15*, 2373.

the distances d_{Si-Hb} and d_{Ru-Si}, and the angles Ru−Hb-Si are the most representative of the activation of the (η^2-H−Si) bonds. However, in the series of the bis(silane) complexes we have reported here, no linear correlation can be drawn between these various parameters. Thus, a correlation of the degree of activation of the Si−H bond with the structural properties and the reactivity of the different compounds is more difficult than in the series of the manganese complexes CpMn(CO)L(η^2-HSiR$_3$). The main difference among our series is between **2**, **3** and **4**−**6**. **3** is by far the most stable as a result of the steric hindrance due to the ring between the two silicons: it is remarkable that no reaction was observed under CO pressure. In contrast **2a,b** show the lowest J_{Si-H} values, are the most reactive, and display the lowest barrier to activation for the hydride exchange process. Theoretical calculations show that the disiloxane isomer analogous to **2** has no symmetry (two Si···H weak interactions), whereas **3**−**6** have symmetric (or almost symmetric) geometries (four Si···H weak interactions). This geometrical contrast could be connected to the difference observed during the reactivity studies. We are presently investigating in more detail this hypothesis, but there is no doubt that the weak nonbonding Si···H interactions play an important role both on the stability and on the reactivity of these σ-complexes. The catalytic properties of these complexes will be reported in due course.

Experimental Section

All reactions and workup procedures were performed under argon using conventional vacuum line and Schlenck tube techniques. All solvents were freshly distilled from standard drying agents and thoroughly degassed under argon before use. Microanalysis were performed by the Laboratoire de Chimie de Coordination Microanalytical Service. Infrared spectra were obtained as Nujol mulls on a Perkin-Elmer 1725 FT-IR spectrometer. NMR spectra were acquired on Bruker AC 200, AM 250, or AMX 400 spectrometers. RuCl$_3$·3H$_2$O was purchased from Johnson Matthey Ltd. The following chemicals were prepared according to published procedures: [RuH$_2$(H$_2$)$_2$(PCy$_3$)$_2$] (**1**),[13e] (Ph$_2$SiH)$_2$O,[40] (Me$_2$SiH)$_2$(CH$_2$)$_3$[41]. The deuterated compound (Me$_2$SiD)$_2$(CH$_2$)$_3$ was made according to the same method as for (Me$_2$SiH)$_2$(CH$_2$)$_3$,[41] but using LiAlD$_4$ instead of LiAlH$_4$. The other silicon products were purchased from Aldrich or ABCR and degassed before use.

Synthesis of [RuH$_2${(η^2-HSiR$_2$)$_2$O}(PCy$_3$)$_2$] (2a,b). (Me$_2$SiH)$_2$O (65 μL, 0.37 mmol) was added at room temperature to a suspension of **1** (122 mg, 0.18 mmol) in pentane (8 mL). Gas evolution was observed immediately. Vigorous stirring was maintained for 2 min during which time the mixture turned orange with formation of a white precipitate. The solid was collected by filtration, washed twice with pentane (2 mL) at 0 °C, and dried under argon and finally under vacuum. Yield, 72%. Anal. Calcd for RuC$_{40}$H$_{82}$OP$_2$Si$_2$: C, 60.12; H, 10.35. Found: C, 59.90; H, 10.38. The same procedure was used for **2b** but with (Ph$_2$SiH)$_2$O (140 mg, 0.37 mmol) and **1** (122 mg, 0.18 mmol). Recrystallization from a toluene/pentane mixture gave analytically pure white crystals of **2b** in 75% yield. Anal. Calcd for RuC$_{60}$H$_{90}$OP$_2$Si$_2$: C, 68.86; H, 8.67. Found: C, 68.65; H, 8.76.

Synthesis of [RuH$_2${(η^2-HSiMe$_2$)$_2$X}(PCy$_3$)$_2$] (3−6). All of these complexes were synthesized by following the same procedure described in detail for [RuH$_2${(η^2-HSiMe$_2$)$_2$(C$_6$H$_4$)}(PCy$_3$)$_2$] (**3**). (Me$_2$SiH)$_2$(C$_6$H$_4$) (65 μL, 0.30 mmol) was added at room temperature to a suspension of **1** (188 mg, 0.28 mmol) in pentane (8 mL). Gas evolution was observed immediately. The stirring was maintained for 15 min during which time a white solid precipitated. The solid was collected by filtration, washed twice with pentane (3 mL) at 0 °C, and dried under vacuum.

(40) Straus, D. A.; Zhang, C.; Quimbita, G. E.; Grumbine, S. D.; Heyn, R. H.; Don Tilley, T.; Rheingold, A. L.; Geib, S. J. *J. Am. Chem. Soc.* **1990**, *112*, 2673.

(41) Bourg, S.; Boury, B.; Carré, F. H.; Corriu, R. J. P. *Organometallics* **1997**, *16*, 3097.

Recrystallization from a benzene/pentane mixture gave analytically pure white microcrystals in 94% yield. Anal. Calcd for RuC$_{46}$H$_{86}$P$_2$Si$_2$: C, 64.37; H, 10.10. Found: C, 64.43; H, 10.48.

[RuH$_2${(η^2-HSiMe$_2$)$_2$(CH$_2$)$_2$}(PCy$_3$)$_2$] (4): Using (**1**) (110 mg, 0.17 mmol) and 2,5-dimethyl-2,5-disilahexane (40 μL, 0.20 mmol). Recrystallization from ether at −20 °C. Yield, 80%. Anal. Calcd for RuC$_{42}$H$_{86}$P$_2$Si$_2$: C, 62.25; H, 10.70. Found: C, 62.14; H, 10.88.

[RuH$_2${(η^2-HSiMe$_2$)$_2$(CH$_2$)$_3$}(PCy$_3$)$_2$] (5): Using (**1**) (180 mg, 0.27 mmol) and 2,6-dimethyl-2,6-disilaheptane (172 μL, 0.81 mmol). (Yield 75%). Anal. Calcd for RuC$_{43}$H$_{88}$P$_2$Si$_2$: C, 62.65; H, 10.76. Found: C, 62.64; H, 10.90.

[RuH$_2${(η^2-HSiMe$_2$)$_2$(OSi(Me$_2$)O)}(PCy$_3$)$_2$] (6): Using (**1**) (300 mg, 0.45 mmol) and 1,1,3,3,5,5-hexamethyltrisiloxane (148 μL, 0.58 mmol). Recrystallization from ether at 20 °C. Yield, 75%. Anal. Calcd for RuC$_{42}$H$_{88}$O$_2$P$_2$Si$_3$: C, 57.82; H, 10.17. Found: C, 57.94; H, 10.27.

Synthesis of [RuH$_2${(η^2-HSiMe$_2$)$_2$X}(PCy$_3$)(PR$_3$). (3Ph, 3pyl, 4Ph, 4pyl). All of these complexes were synthesized by following the same procedure described for [RuH$_2${(η^2-HSiMe$_2$)$_2$(C$_6$H$_4$)}(PCy$_3$)(PPh$_3$)] (**3Ph**). A pentane solution (5 mL) of triphenylphosphine (37 mg, 0.14 mmol) was added to a suspension of [RuH$_2${(η^2-HSiMe$_2$)$_2$(C$_6$H$_4$)}-(PCy$_3$)$_2$] (**3**) (90 mg, 0.11 mmol) in pentane (10 mL). The mixture was stirred for 24 h at room temperature. A white precipitate was then collected by filtration, washed twice with pentane (3 mL), and dried under vacuum. Yield, 80%. Anal. Calcd for RuC$_{46}$H$_{68}$P$_2$Si$_2$: C, 65.76; H, 8.16. Found: C, 65.24; H, 9.01.

[RuH$_2${(η^2-HSiMe$_2$)$_2$(C$_6$H$_4$)}(PCy$_3$)(Ppyl$_3$)] (3pyl): Using (**3**) (150 mg, 0.17 mmol) and tripyrrolylphosphine (48 mg, 0.21 mmol). Yield, 70%. Anal. Calcd for RuC$_{40}$H$_{65}$N$_3$P$_2$Si$_2$: C, 59.52; H, 8.12; N, 5.21. Found: C, 58.74; H, 8.44; N, 5.02.

[RuH$_2${(η^2-HSiMe$_2$)$_2$(CH$_2$)$_2$}(PCy$_3$)(PPh$_3$)] (4Ph): Using (**4**) (110 mg; 0.14 mmol) and triphenylphosphine (58 mg, 0.22 mmol). Yield, 86%. Anal. Calcd for RuC$_{42}$H$_{68}$P$_2$Si$_2$: C, 63.68; H, 8.65. Found: C, 63.42; H, 8.80.

[RuH$_2${(η^2-HSiMe$_2$)$_2$(CH$_2$)$_2$}(PCy$_3$)(Ppyl$_3$)] (4pyl): Using (**4**) (100 mg, 0.12 mmol) and tripyrrolylphosphine (26 mg, 0.12 mmol). Yield, 75%. Anal. Calcd for RuC$_{36}$H$_{65}$N$_3$P$_2$Si$_2$: C, 56.96; H, 8.63; N, 5.54. Found: C, 56.29; H, 8.31; N, 5.19.

Synthesis of [RuH$_2${(η^2-HSiMe$_2$)$_2$X}(PR$_3$)$_2$]. (3Ph$_2$, 3pyl$_2$, 4Ph$_2$, 4pyl$_2$). All of these complexes were synthesized by following the same procedure described for [RuH$_2${(η^2-HSiMe$_2$)$_2$(C$_6$H$_4$)}(PPh$_3$)$_2$] (**3Ph$_2$**). Ru(COD)(COT) (100 mg; 0.32 mmol), triphenylphosphine (138 mg, 0.53 mmol), and 1,2-bis-dimethylsilylbenzene (100 μL, 0.46 mmol) were introduced into a Fischer−Porter bottle, and dichloromethane (10 mL) was added. The bottle was pressurized to 3 bar of dihydrogen. The solution was stirred for 2 h at room temperature and then evaporated to dryness. The residue was washed several times with pentane, affording a white solid which was then dried under vacuum. Yield, 86%. Anal. Calcd for RuC$_{46}$H$_{50}$P$_2$Si$_2$: C, 63.68; H, 8.65. Found: C, 63.42; H, 8.80.

[RuH$_2${(η^2-HSiMe$_2$)$_2$(C$_6$H$_4$)}(Ppyl$_3$)$_2$] (3pyl$_2$): Using Ru(COD)(COT) (100 mg; 0.32 mmol), tripyrrolylphosphine (142 mg, 0.62 mmol) and 1,2-bis-dimethylsilylbenzene (70 μL, 0.32 mmol). Yield, 70%. Anal. Calcd for RuC$_{34}$H$_{44}$N$_6$P$_2$Si$_2$: C, 54.02; H, 5.87; N, 11.12. Found: C, 55.03; H, 5.56; N, 11.70.

[RuH$_2${(η^2-HSiMe$_2$)$_2$(CH$_2$)$_2$}(PPh$_3$)$_2$] (4Ph$_2$): Using Ru(COD)(COT) (104 mg, 0.33 mmol), triphenylphosphine (169 mg, 0.64 mmol) and 2,5-dimethyl-2,5-disilahexane (90 μL, 0.46 mmol). Yield, 82%. Anal. Calcd for RuC$_{42}$H$_{50}$P$_2$Si$_2$: C, 65.17; H, 6.51. Found: C, 64.54; H, 6.57.

[RuH$_2${(η^2-HSiMe$_2$)$_2$(CH$_2$)$_2$}(Ppyl$_3$)$_2$] (4pyl$_2$): Using Ru(COD)(COT) (98 mg, 0.31 mmol), tripyrrolylphosphine (134 mg, 0.59 mmol) and 2,5-dimethyl-2,5-disilahexane (80 μL; 0.41 mmol). Yield, 71%. Anal. Calcd for RuC$_{30}$H$_{38}$N$_6$P$_2$Si$_2$: C, 51.40; H, 5.42; N, 11.98. Found: C, 51.00; H, 5.45; N, 11.84.

Synthesis of [RuH$_2$(ᵗBuNC)$_2$(PCy$_3$)$_2$] (8). ᵗBuNC (50 μL, 0.45 mmol) was added at room temperature to a suspension of **1** (150 mg, 0.23 mmol) in pentane (8 mL). Gas evolution was observed immediately. The resulting orange solution was concentrated to 4 mL leading to the formation of a white precipitate. The solid was collected by filtration and washed twice with pentane (3 mL) and dried under

vacuum. Yield, 92%. Anal. Calcd for $RuC_{46}H_{86}N_2P_2$: C, 66.55; H, 10.44; N, 3.37. Found: C, 66.26; H, 10.85; N, 3.31.

Synthesis of [RuH₂(H₂)(PCy₃)₂(Ppyl₃)] (9). A pentane solution (4 mL) of tripyrrolylphosphine (69 mg, 0.30 mmol) was added at room temperature to a suspension of **1** (210 mg, 0.31 mmol) in pentane (8 mL). The resulting orange mixture was stirred for 15 min leading to the formation of a white precipitate. The solid was collected by filtration, washed twice with pentane (3 mL), and dried under vacuum. Yield, 71%. Anal. Calcd for $RuC_{48}H_{82}N_3P_3$: C, 64.41; H, 9.23; N, 4.69. Found: C, 63.95; H, 8.92; N, 4.64.

Synthesis of [RuH₂(Ppyl₃)₄] (10): Same procedure as for **1** but using Ru(COD)(COT) (100 mg, 0.32 mmol) and tripyrrolylphosphine (330 mg, 1.44 mmol). Recrystallization from CH_2Cl_2 at -20 °C. Yield, 90%. Anal. Calcd for $RuC_{48}H_{50}N_{12}P_4$: C, 56.55; H, 4.95; N, 16.49. Found: C, 56.29; H, 5.31; N, 16.19.

X-ray Structure Determination. For all compounds, data were collected on a Stoe IPDS (imaging plate diffraction system) equipped with an Oxford Cryosystems cooler device. The crystal-to-detector distance was 80 mm. Crystal decay was monitored by measuring 200 reflections per frame. The final unit cell parameters were obtained by least-squares refinement of 5000 reflections. Only statistical fluctuations were observed in the intensity monitors over the course of the data collections. Numerical absorption corrections were applied for all complexes.

The five structures were solved by direct methods (SIR92)[42] and refined by least-squares procedures on F_{obs}. H atoms were located on difference Fourier syntheses, but those attached to carbon were introduced in calculation in idealized positions (d(CH) = 0.96 Å), and their atomic coordinates were recalculated after each cycle. They were given isotropic thermal parameters 20% higher than those of the carbon to which they are attached. The coordinates of hydrides H were refined with an equivalent isotropic thermal parameter. Least-squares refinements were carried out by minimizing the function $\Sigma w(|F_o| - |F_c|)^2$, where F_o and F_c are the observed and calculated structure factors. The weighting scheme used in the last refinement cycles was $w = w'[1 - \{\Delta F/6\sigma(F_o)\}^2]^2$ where $w' = 1/\Sigma_1^n A_r T_r(x)$ with three coefficients A_r for the Chebyshev polynomial $A_r T_r(x)$ where x was $F_c/F_c(\text{max})$.[43] Models reached convergence with $R = \Sigma(||F_o| - |F_c||)/\Sigma(|F_o|)$ and $R_w = [\Sigma w(|F_o| - |F_c|)^2/\Sigma w(F_o)^2]^{1/2}$, having values listed in Table 3.

The calculations were carried out with the CRYSTALS package programs.[44] The drawing of the molecule was realized with the help of ORTEP3.[45] Complete crystal data, fractional atomic coordinates and the equivalent thermal parameters for all atoms, anisotropic thermal parameters for non-hydrogen atoms, and a full list of bond lengths and bond angles have been deposited at the Cambridge Crystallographic Data Center.

Computational Details

All calculations were performed with the Gaussian 94 suite of programs.[46] For ruthenium, the core electrons were represented by the relativistic small-core pseudopotential employed in our previous calculations on $RuH_2(H_2)(PH_3)_2$.[13h] The 16 electrons corresponding to the 4s, 4p, 4d, and 5s atomic orbitals were described by a (8s, 6p, 6d) primitive set of Gaussian functions flexibly contracted to [5s, 5p, 3d]. Standard pseudopotentials developed in Toulouse[47] were used to describe the atomic cores of all other non-hydrogen atoms (Si, P, C, and O). A double-ζ plus polarization valence basis set was employed for each atom (d-type function exponents were 0.45, 0.45, 0.80, and 0.85, respectively). For hydrogen, a standard primitive (4s) basis contracted to [2s] was used. A p-type polarization function, exponent 0.9, was added for the four hydrogen atoms directly bound to ruthenium (H1, H2, Hb1, and Hb2). Pure spherical harmonic functions were used throughout.

All stationary points of interest were located at the B3LYP level of theory, a density functional theory (DFT) type of calculation based on hybrid functionals, which we have shown to perform well in our earlier computational study of **1**.[13h] Analytical first derivatives of the energy were used to optimize geometrical parameters, and frequency calculations were performed to determine whether the optimized geometries were minima on the potential energy surface. Most of these calculations were also performed with the B3PW91 functional which uses the correlation functional of Perdew and Wang (PW),[48] instead of that due to Lee, Yang, and Parr (LYP).[49] The exchange functional due to Becke (B) is adopted in both cases.[50]

Supporting Information Available: Tables of more extensive computational results, 400 MHz ^{1}H NMR spectra of **4pyl** in C_6D_6 showing selective ^{31}P decouplings, X-ray structural information on **3**, **4**, **4Ph**, **4Ph₂**, and **6** (PDF). This material is available free of charge via the Internet at http://pubs.acs.org.

JA990199J

(42) Altomare, A.; Cascarano, G.; Giacovazzo, G.; Guagliardi, A.; Burla, M. C.; Polidori, G.; Camalli, M. *SIR92*-a program for automatic solution of crystal structures by direct methods, *J. Appl. Crystallogr.* **1994**, *27*, 435.

(43) Prince, E. *Mathematical Techniques in Crystallography*; Springer-Verlag: Berlin, 1982.

(44) Watkin, D. J.; Prout, C. K.; Carruthers, J. R.; Betteridge, P. W. *CRYSTALS Issue 10*, Chemical Crystallography Laboratory, University of Oxford, Oxford, 1996.

(45) ORTEP3 for Windows. Farragia, L. J. *J. Appl. Crystallogr.* **1997**, *30*, 565.

(46) Gaussian 94, Frisch, M. J.; Trucks, G. W.; Schlegel, H. B.; Gill, P. M. W.; Johnson, B. G.; Robb, M. A.; Cheeseman, J. R.; Keith, T. A.; Petersson, G. A.; Montgomery, J. A.; Raghavachari, K.; Al-Laham, M. A.; Zakrzewski, V. G.; Ortiz, J. V.; Foresman, J. B.; Cioslowski, J.; Stefanov, B. B.; Nanayakkara, A.; Challacombe, M.; Peng, C. Y.; Ayala, P. Y.; Chen, W.; Wong, M. W.; Andres, J. L.; Replogle, E. S.; Gomperts, R.; Martin, R. L.; Fox, D. J.; Binkley, J. S.; Defrees, D. J.; Baker, J.; Stewart, J. P.; Head-Gordon, M.; Gonzalez, C.; Pople, J. A. Gaussian, Inc, Pittsburgh, PA, 1995.

(47) Bouteiller, Y.; Mijoule, C.; Nizam, M.; Barthelat, J.-C.; Daudey, J. P.; Pélissier, M.; Silvi, B. *Mol. Phys.* **1988**, *65*, 2664.

(48) Perdew, J. P.; Wang, Y. *Phys. Rev. B*, **1992**, *45*, 13244.

(49) Lee, C.; Yang, W.; Parr, R. G. *Phys. Rev. B*, **1988**, *37*, 785.

(50) Becke, A. D. *J. Chem. Phys.*, **1993**, *98*, 1372 and 5648.